Invited paper

Characterization and Modeling of Pores and Surfaces in Cement Paste: Correlations to Processing and Properties

Hamlin M. Jennings[1,2], Jeffrey W. Bullard[3], Jeffrey J. Thomas[1], Jose E. Andrade[1], Jeffrey J. Chen[4] and George W. Scherer[5]

Received 12 December 2007, revised 25 January 2008

Abstract

Cement-based materials have complex multi-component, multiscale structures that first form through chemical reaction and then continue to change with time. As with most classes of materials, the porosity of cement paste strongly influences its properties, including strength, shrinkage, creep, permeability and diffusion. Pores in cement paste range in size from nanometers to millimeters, and numerous investigations and models have been reported in the literature. This paper reviews some key concepts and models related to our understanding of the pore system and surface area. A major reason for the complexity of cement-based materials is that the principal reaction product, calcium silicate hydrate (C-S-H), forms with a significant volume fraction of internal, nanometer-scale pores. This gel pore system contains water that is also adsorbed to the solid surfaces, blurring the distinction between the solid phase and pores. The gel pore system changes not only with the chemical composition and extent of reaction, but also with changes in relative humidity, temperature, and applied load. Pores can be characterized by their surface area, size, volume fraction, saturation, and connectivity, but precise quantitative models are still not available. A useful approach for characterizing the structure of cement paste is to document the influence of time and external factors on structural changes. Scientific progress will be facilitated by the development of models that accurately describe the structure and use that structure to predict properties. This is particularly important because the composition and chemistry of commercial concretes is changing more rapidly than laboratory experimentation can document long-term properties such as durability. Some of the possible models are discussed.

1. Introduction

A primary aim of materials science is to establish quantitative relationships between processing, structure, and properties. For metals, ceramics, and polymers this has been accomplished with mathematical models based on fundamental principles that can be used to predict or design their properties. For concrete, one of the world's most important and widely studied technological materials, the processing-structure-property relationships are extremely complex. Concrete is a multiscale, multicomponent material, containing particles of coarse aggregate (approximately 10 mm to 100 mm diameter) and sand (approximately 0.01 mm to 2 mm diameter), suspended in a cement paste binder, a multiphase suspension of cement and fillers (0.1 μm to 100 μm diameter) mixed with water. The most important component of concrete is cement paste, which itself is composed of several phases. For cement paste, a schematic of the materials science approach is shown in **Fig. 1**, and, as will be argued, the complexity and sheer number of important properties presents significant challenges to the formulation of the desired models. The purpose of this paper is to enumerate these challenges by reviewing the state of knowledge regarding the pore system of cement paste, by describing how modern numerical modeling tech-

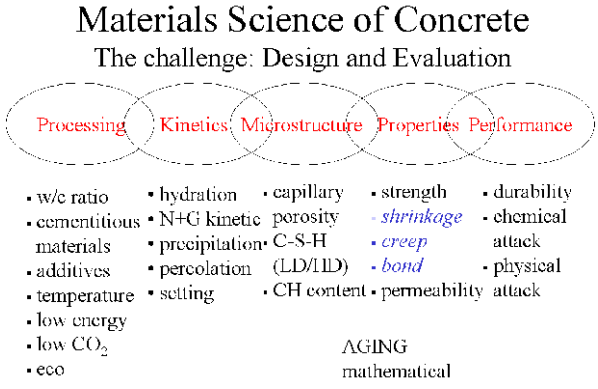

Fig.1 Processing-structure-property-performance relationships for concrete.

[1]Department of Civil and Environmental Engineering, Northwestern University, Evanston, IL USA.
[2]Department of Materials Science and Engineering, Northwestern University, Evanston, IL USA.
E-mail:h-jennings@northwestern.edu
[3]Materials and Construction Research Division, National Institute of Standards and Technology , Gaithersburg, MD USA.
[4]Lafarge Centre de Recherche, St Quentin Fallavier, France.
[5]Civil & Environmental Engineering, Princeton University, Dept. Civil & Env. Eng/PRISM, Princeton Univeresity, Princeton, NJ USA.

niques can address outstanding issues regarding the development of the complex hydrated microstructure, and by showing how predictions of mechanical and transport properties can be made from this microstructure. Suggestions are then made as to how future models might be directed to overcome the remaining challenges.

Structurally, cement paste is a dense suspension of particles in a liquid medium, and the liquid component can be viewed as a three-dimensional pore space between the solid particles. The pore structure and the aqueous phase it contains, which we refer to collectively as the *pore system*, is a major part of the cement paste structure, bridging length scales from nanometers to millimeters, and controlling many important engineering properties. A premise of this paper is that the pore system is a key characteristic linking processing, structure, and properties, and is therefore an appropriate focus for modeling efforts. In this paper, we will specifically discuss new approaches to modeling the changes to the pore system with time under different conditions (Section 5.3), and to modeling the influence of the pore system on the mechanical properties of concrete (Section 5.4).

Despite its central role in the behavior of cementitious materials, and despite the fact that precise characterization of the pore system in cement paste has been the subject of research for more than half a century, we still do not have rigorous definitions of different pore types or a full geometric description of the pore system. Therefore, models representing the current state of the art are still incomplete, and none can adequately predict performance over a wide range of mineral and chemical formulations. The issue of performance as a function of chemical composition is becoming increasingly important as the range of materials utilized as binder materials in concrete widens, driven by the need to reduce energy consumption and greenhouse gas emissions associated with cement production (Gartner 2004, Damtoft *et al*. 2008). For example, the pore system of cement pastes containing slag, fly ash, and other materials is known to be different from that of Portland cement paste (Richardson 2004, Chen 2006), but the corresponding changes in concrete properties cannot be reliably predicted by present models.

The ideal concrete model might be envisioned as a sophisticated but user-friendly computer program that takes as its input the desired engineering properties of the concrete and the expected environmental conditions in the field and then, after accessing an extensive database of available cementitious materials and admixtures, and performing a series of comprehensive simulations, outputs detailed instructions for materials selection, mixture proportioning, and processing such a concrete. The realization of this type of program is some distance in the future, but it is argued here that significant advances in concrete modeling may occur in the next few years (Bullard 2004).

The organization of this paper is as follows. In Section 2, we survey the state of knowledge of the pore system in cement paste, and of how the pore system relates to material properties, following to some extent a historical perspective. In Section 3, we discuss the curing process, including some recent insight obtained into the details of the hydration kinetics. In Section 4, we review some of the recent data obtained regarding the pore system of cement paste using advanced characterization methods. Then, in Section 5, we turn to modeling, focusing on two promising new strategies for modeling the development of structure and the relationships between structure and mechanical properties. Finally, in Section 6, some general and concluding remarks are given. We note that there are characterization techniques and models of excellent quality that are not referred to here. An intention of this paper is to describe relationships between experimental characterization and models that have advanced, and are likely to continue advancing, our understanding and control of cement based materials.

2. Historical survey of the pore system in concrete

When cement powder and water are mixed, reactions begin to consume the cement particles and to produce solid products. This is accompanied by a net decrease in volume, called chemical shrinkage, because the volume of the solid products of hydration is less than the initial volume of solids and water from which they form. However, the solid hydration products have greater volume than the initial solids alone, so the water filled space is gradually replaced by solids during the reaction. The space not filled by solid products of hydration is traditionally called the capillary pore space. The principal hydration product, calcium silicate hydrate (C-S-H) gel, also contains a significant volume of very small pores called gel pores. In this sense, the pore system naturally divides into two distinct populations of pores, one population becoming less numerous, and the other becoming more numerous, as the reactions proceed. This fundamental classification system for porosity in cement paste is one of the oldest (Powers and Brownyard 1948), but it is perhaps most easily illustrated by a micrograph showing the simulated microstructure generated by a modern computer model at two hydration times (**Fig. 2**). At first, the capillary pores form a simply connected topological space in three dimensions. However, as hydration proceeds, the capillary pore volume decreases continuously until, at some point, it may transform into a disconnected space by a percolation transition (Garboczi and Bentz 2001). This depercolation has significant effects on the material's transport properties (Powers 1959, Bentz 2007).

While dividing the pore system into capillary and gel components based on the hydration process is attractive, in practice it should be noted that there is an overlap in these two subsystems in the range of about 5 nm to 20

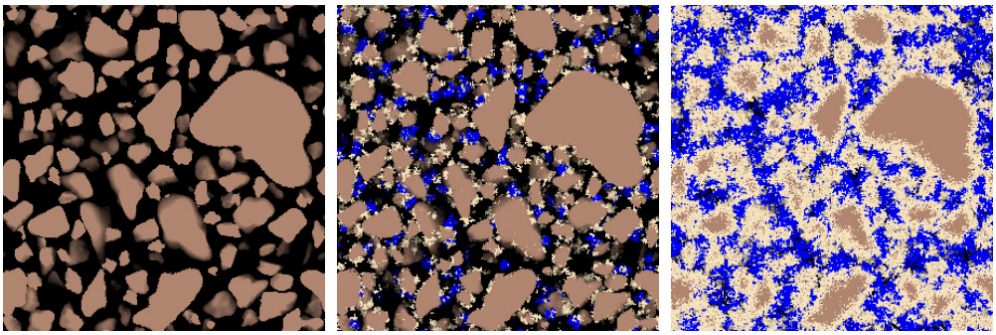

Fig.2 Two-dimensional cross-sections from a simulated three-dimensional microstructure of C_3S paste with water/cement = 0.5 at degrees of hydration of 0, 0.1, and 0.6 (left to right). Images were generated using the VCCTL microstructure model (Bullard and Garboczi 2006). The colors are as follows: black = saturated capillary porosity, dark brown = C_3S, light brown = C-S-H including gel pores, blue = CH.

nm. Knowledge about the structure of pores in these two populations historically has resulted not only from direct measurements, but also from inferences based on the macroscopic response of the material. In this spirit, we review the capillary and gel pore systems principally in terms of the engineering properties that are most influenced by change of the pore structure at those length scales.

2.1 Relation of capillary pores to cement paste properties

For both engineering and practical reasons, compressive strength is the most commonly measured property that relates directly to capillary pores. A number of early models related strength to various measures of pore structure. The first of these was Feret's Law (Feret 1897):

$$\sigma = K\left(\frac{c}{c+w+a}\right)^2 \tag{1}$$

where σ=compressive strength, K=constant, c=volume of cement, w=volume of water, a=volume of air.

This is an empirical relationship that effectively relates the amount of water in the original mix to the ultimate strength. Since the ratio of water to cement is directly related to the capillary pore volume, it can be seen that the qualitative relationship between porosity and strength was firmly established more than 100 years ago. Over the years, at least a half dozen different multiparameter equations have been found to provide good correlations between porosity, appropriately defined, and compressive strength (Ryshkewitch 1953).

Powers (1960), who might be considered the first modern cement researcher, recognized the importance of the larger capillary pores, and the tendency for their volume to decrease with increasing degree of hydration. To model compressive strength, he developed the concept of the gel/space ratio, X , defined as the volume of solid hydration products and associated small pores, referred to collectively as *gel*, divided by the total volume of the paste. This quantity can be fit to strength data using two unknown constants, A and n:

$$\sigma = AX^n \tag{2}$$

This relationship accounts for the effects of the degree of reaction and the original water cement ratio on strength through the calculation of X. Eqs. 1 and 2 both reflect the experimental fact that reducing capillary porosity tends to increase the strength.

Implicit in the Powers interpretation (Eq. 2), based on the assumption of a fixed amount of non-evaporable water, is the assumption that the volume fraction of gel pores in C-S-H is constant (Powers 1960, Powers 1958, Taylor 1997) such that C-S-H gel, including solid and gel pore, has a constant specific volume. A recent model of the nanostructure of C-S-H (Jennings 2000, Jennings 2008) questions this assumption, proposing instead that the volume fraction of gel pores in C-S-H takes on two local values, one for a high-density packing and one for a low-density packing of nanoscale solid C-S-H particles. At the scale of hundreds of nanometers, the C-S-H phase would have a distribution of packing densities around these two values, a prediction that has experimental support from nanoindentation measurements (Constantinides and Ulm 2004). Since the lower density morphology of C-S-H is favored at earlier ages, this means that the specific volume of C-S-H decreases with time. Other variables such as curing temperature, drying (autogenous and external), and loading could affect the packing efficiency of the C-S-H building blocks, a phenomenon known generally as aging (Bazant 2001). The capillary porosity, and thus the strength, will thus depend on the full environmental history of the paste and not just the degree of reaction and initial water:cement mass ratio (w/c). For example, the strength of a paste was found to depend on drying and load history when the overall degree of reaction and w/c were kept constant (Garrett *et al*. 1979). Since drying causes cracking, especially in larger samples where moisture gradients are inevitable, and cracking decreases strength, relationships between moisture content, capillary pores, and strength are much more complicated than is implied by the simple empirical relationships of Eqs. (1) and (2).

Characterizing the changes that occur as a result of aging represents a major challenge that is taken up in more detail in a later section.

The mechanical properties of cement paste are not the only properties affected by the capillary porosity. The permeability of cement paste, which is generally defined as the ease with which the aqueous phase flows through the material under a pressure gradient, is also directly related to the volume, size, and morphology of capillary pores. However, the measured permeability of a mature cement paste tends to be much smaller than the value predicted from the measured pore size distribution (Scherer *et al.* 2007, Vichit-Vadakan Scherer 2000). These authors examined the applicability of a variety of models for permeability of cement paste. The agreement between calculated and measured permeabilities for cement paste or concrete is generally poor, but this is likely due to the use of pore sizes measured on dried samples. Because drying causes microcracking and other changes, the measured pores are larger than in the virgin samples used to measure permeability; consequently, the calculated permeability is too high, unless a very large tortuosity is assumed. On the other hand, when dried cement is resaturated, its permeability is found to be 100 times higher than in the virgin samples (Powers *et al.* 1955), presumably because of larger pores formed during the drying process, but there are no studies in which the measured pore size is used to analyze the permeability of resaturated samples (which would be the appropriate comparison). For materials that are much simpler than cement, such as porous Vycor glass, the permeability is accurately described by the Kozeny-Carman equation, if the presence of an immobile monolayer of solvent is taken into account (Vichit-Vadakan and Scherer 2000). If an immobile solvent layer is also used to deduce the pore size of cement paste based on permeability measurements, the pore diameter is found to be 1.5 nm to 5 nm, as shown in **Fig. 3**. These pore sizes are in the range expected for the gel pores, and correspond fairly well to the sizes measured by nuclear magnetic resonance spectroscopy (NMR) relaxation time analysis. This suggests that the much larger capillary pores, which are present when the measurement is made, are depercolated and therefore do not participate in fluid flow.

2.2 Gel pores and interlayer space

While capillary pores are defined rather indirectly as the residual water filled space that remains as the reaction products expand, the gel pores are specifically associated with the C-S-H gel phase, which is the primary hydration product of all portland cement based cementitious materials. At an even smaller scale, there are also interlayer spaces between the Ca–O sheets of C-S-H where H_2O molecules can reside. These are not technically pores since they do not contain liquid, but in practice the distinction between interlayer space and gel porosity is also ambiguous as adsorbed water in the gel pores and interlayer water are removed simultaneously during drying. For this reason, characterization of gel pores has proven to be one of the most contentious issues in concrete science even though these pores are central to several important properties. Gel pores are responsible for the extremely high surface area of C-S-H, and they contain adsorbed water that plays a critical role in drying shrinkage and creep. This means that the properties associated with gel pores are also controlled by the surface energy of C-S-H.

An extremely important property of concrete is the volume strain associated with changes in its water content, which are induced by changes in the relative humidity of its environment. This phenomenon is generally referred to as drying shrinkage. When the shrinkage is restrained, which in concrete structures is unavoidable, cracking can occur with an associated deterioration in properties. From a research point of view, much of the early progress on modeling the structure of the hydration products resulted from interpreting measurements of length changes that occur on drying and resaturation. All of these models revolve around the structure and thermodynamics of the pores and associated surface area. Between the 1940's and the 1960's, much was learned about the interaction of liquids and gases with high surface area particulate solids, a class of materials known as colloids. Inspired by the research of Brunauer, Emmett and Teller (1938), adsorption isotherms using water vapor, nitrogen, and other gases were used to determine the specific surface area of cement paste. While the value in all cases was very high, different gases pro-

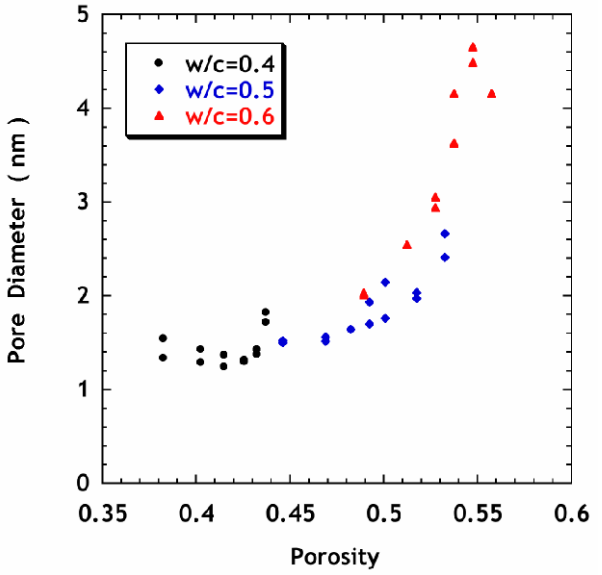

Fig. 3 Pore sizes calculated from the Carman-Kozeny equation using permeabilities measured on Type III cement paste (Vichit-Vadakan and Scherer 2000, 2004). The pores are assumed to contain a layer of water 0.5 nm thick that is immobilized on the pore wall, so the effective diameter through which flow occurs is 1 nm smaller than the value shown.

duced quite different values (Thomas *et al*. 1998). To this day there are disagreements on how to interpret the surface area results in terms of modeling the gel pore structure and C-S-H nanostructure.

Using water as an adsorbate, the adsorption isotherm for cement paste behaves as if a monolayer forms on the surface of the solid gel at 11 % relative humidity (RH). **Figure 4**, which shows the length change of a paste specimen as a function of weight loss on drying**,** is a composite of a number of water sorption isotherms that highlights some of the observations that should be quantitatively captured in a model of the microstructure. The first drying and rewetting cycle, indicated by the top curve and solid red curve, respectively, imposes a permanent loss in length of the specimen indicated by the difference in the two curves at 100 % RH, which is known as irreversible shrinkage. While subsequent cycles do not generally result in further irreversible shrinkage, a large hysteresis is observed during every cycle of drying and rewetting. Thus, the microstructure has some intrinsic hysteretic properties. Sorption isotherms performed using nitrogen (a slightly larger molecule than water) do not show the low pressure hysteresis, and imply lower values of specific surface area than when water is used as the adsorbate. These results formed the basis of much of the modeling of the structure of the hydration products in the 1950's and 1960's, as described in the following section.

2.3 The Powers and Brownyard model of pore structure and shrinkage

During the 1940's, Powers and Brownyard (1948) introduced several concepts that to this day form the basis of our understanding of the pore system in cement based materials. They were the first to explore structure by attempting to establish relationships between structure and properties. They measured "*water fixation in hardened portland cement paste, the properties of evaporable water, the density of the solid substances, and the porosity of the paste as a whole*." They considered the reaction products to be colloidal in nature, and referred to them collectively as the "cement gel." Adsorption experiments indicated that the gel had an extremely high surface area, particularly as measured by water, and therefore that C-S-H must have significant internal porosity. The density was also measured by water (Archimedes method) and by determining the minimum w/c necessary for complete hydration. This led them to calculate that the minimum volume fraction of gel pores in the hydration products was 28 %. This value, which provides a clear distinction between gel and capillary pores, remains central to all models of porosity in cement paste.

As described in the previous section, C-S-H surface area values inferred from nitrogen adsorption are lower than those inferred from water adsorption, although the nitrogen values are sensitive to the method used to dry the specimen prior to the measurement. Furthermore,

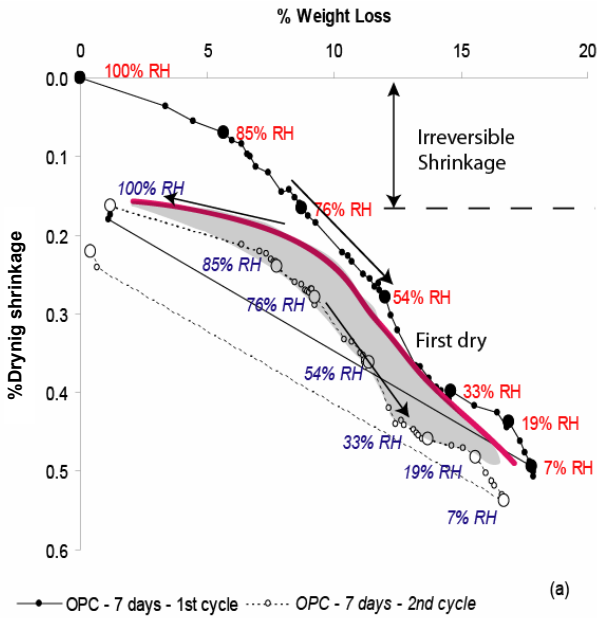

Fig. 4 Length change vs weight loss for cement paste. This figure is a composite representing the results from several researchers. The desorption data comes from Jennings (2008) and the adsorption from (Ramachandran *et al*. 1981). The weight loss as a function of relative humidity provides information about size distribution of pores, and length change provides data that is useful to models relating nanostructure to shrinkage (see section 4.3)

while water adsorption/desorption isotherms exhibit large hysteresis, the nitrogen isotherms are essentially reversible (i.e., no hysteresis between drying and wetting). Powers and his colleagues explained these data by suggesting that nitrogen cannot enter the smallest pores because their entrances are smaller than their diameter (so-called "ink bottle" pores), and that the extent to which these entrances block the nitrogen molecule depends on the drying treatment.

Powers (1968), and Powers and Brownyard (1948) analyzed the relationship between volume of pores, water content, dimensional change, strength and a few other properties including resistance to freezing and thermal expansion. Drying shrinkage has proven to be a particularly challenging property to understand and model. According to Powers (1968): "*A solid body composed of particles and interstitial spaces i.e. pores, may undergo a change of volume if: 1) the specific volume (or density) of the material which the particles are composed changes; or if 2) the body is compressed or dilated in such a way as to reduce or increase the porosity or if (1) and (2) both kinds of change occur together.*"

The first change occurs if water is removed from the surface of particles to change surface energy:

$$\frac{\Delta V}{V} = \frac{2RT}{3KM}\int_{h_1}^{h_2} \frac{w_a}{b} d\ln h \tag{3}$$

where V= volume, R= universal gas constant, K= bulk modulus of solid, later referred to as K_s, M= molecular weight of water, h=relative humidity, w_e= weight of evaporable adsorbed water at h, b= weight of solid component.

This is a version of the Bangham equation (Bangham 1946), which is a basic model relating changes in surface tension (energy) due to loss of water to volume changes. Because the particles in question have nanoscale dimensions, Eq. 3 provides a relationship between nanostructure and properties, which explores mechanisms of volume change. Powers tried to use this equation to model drying shrinkage but he was only able to demonstrate that the change in surface tension of the solid by adsorption of water was too small to explain the observed shrinkage in cement paste (Powers 1968). Even though his model of drying shrinkage, Eq. 3, did not agree with experiment, his approach demonstrated the power of formulating a model, checking its consequences against experimental observations, and possibly reformulating the model to obtain better understanding and agreement with experiment. This remains the best approach to understanding new materials. Actually, changes in surface energy are greatest during desorption at lower RH values, and therefore the Bangham effect is most pronounced at lower RH values.

A somewhat similar phenomenon, relating changes in surface energy to changes in volume, is disjoining pressure. Disjoining pressure is the pressure in a thin layer of liquid between two closely-spaced solid surfaces, which tends to push the solids apart. This pressure is caused by the reduction in free energy when the liquid layer thickens. Powers argued that disjoining pressure takes on essentially the same form and has the same sign as Eq. 3, so that the volumetric strain is actually the sum of two similar terms and can be described by

$$\frac{\Delta V}{V} = \frac{f(w)RT}{MK_c}\int_{h_1}^{h_2} d\ln h \tag{4}$$

where $f(w)$ =fraction of cross section where disjoining operates, K_c = bulk modulus of gel and pore system.

The importance of disjoining pressure continues to be a subject of interest (Beltzung and Wittmann 2005). While it is frequently stated that this term does not become important until above 50% RH, this model should be further evaluated with data at lower RH values. Another way of looking at disjoining pressure is that it may be important to swelling during adsorption at higher relative humidities when a meniscus has not yet formed, as opposed to drying when a meniscus is present. Again, this is a model that is useful for exploring mechanisms by which nanostructure affects bulk properties.

Most of the dimensional change observed when drying from saturation to about 50 % RH, the range of greatest practical importance for cement based materials, is associated with capillary stress in the liquid as the air-water interface forms a meniscus and the larger pores empty. Pores larger than about 2 nm are empty in this RH range. While a precise expression for deformation of saturated porous systems has been published (Coussy 2004), one of the challenges of poromechanics is to compute bulk volumetric strain of a partially saturated porous material. This has been the subject of recent research (Coussy *et al*. 2004) and relationships with the following form, which have existed for decades (Mackenzie 1950), have been discussed in the literature (Bentz *et al*. 1998):

$$\frac{\Delta V}{V} = p\left(\frac{1}{K} - \frac{1}{K_s}\right)S \tag{5}$$

where K=bulk modulus of porous system, K_s= bulk modulus of solid skeleton, S= degree of saturation, $p = \frac{RT}{M}\ln(h)$.

This formulation, applicable both to external drying shrinkage and to autogenous shrinkage, is significantly different from the one first developed by Powers (1968), and can be based on rigorous mechanics when the pore space is completely filled (S = 1). The role of the solid and of the solid plus pores is explicitly accounted for, and the pressure is reduced by a factor S, which has the effect of averaging the pressure over all of the pores, filled or not. These equations can provide insight and are the subject of continuing research (Vlahinic *et al*. 2008). Understanding porosity is central to understanding volume changes on drying, and if models that predict porosity are developed then properties can be designed from first principles.

Powers and Brownyard (1948) used this type of analysis to deduce that C-S-H is an assemblage of particles about 3 nm to 4 nm in size, and that surface energy and interparticle forces are the major cause of dimensional change during drying. Their problem was that the data and theory did not agree under detailed analysis. This is clearly a complex issue requiring further research.

2.4 New information in the 1950's and 1960's – C-S-H structure and water

During the 1950's and 1960's, an enormous amount of new information about the hydration products of cement paste was published (Taylor 1950, Taylor 1961, Taylor 1968, Feldman and Sereda 1968). Most importantly, the products of hydration were separated into distinct phases and the principal product, calcium silicate hydrate gel, was studied separately. This gel eventually assumed the name C-S-H, where the dashes indicate that exact quantities of each component could vary.

H.F.W. Taylor (Taylor 1961) was the first to point out that C–S–H has a well-defined short range order that resembles the structure of crystalline calcium silicate hydrate minerals such as tobermorite. Further work (Taylor 1968) suggested that disordered forms of the

minerals 1.4-nm tobermorite ($Ca_5Si_6O_{16}(OH)_2 \cdot 7H_2O$) (Bonaccorsi *et al.* 2005) and jennite ($Ca_9Si_6O_{18}(OH)_6 \cdot 8H_2O$ (Bonaccorsi *et al.* 2004) were the most promising models for C–S–H in cement paste (Taylor 1986). Both 1.4-nm tobermorite and jennite are based on a composite layer structure, comprised of infinite Ca–O sheets, ribbed with silicate chains that repeat every 3 tetrahedral units (i.e. dreierketten). This particular configuration of the silicate chains is imposed by the interatomic spacing of the Ca–O sheet. Between the composite layers lie interlayer Ca ions and associated water molecules (see **Fig. 5**). Upon dehydration, the loss of these interlayer water molecules generally induces a decrease in the layer spacing, which for tobermorite ranges from 1.4 nm to 0.9 nm. In this respect, C–S–H compounds are similar to clay minerals, except that the silica moieties are infinite chains instead of sheets.

Knowledge of the structure of C–S–H has great practical importance because mechanical responses of concrete such as shrinkage and creep are directly tied to the nature of the molecules trapped in the interlayer spaces and in the larger pore spaces between the crystalline domains. Some insights about the water associated with C–S–H can be gained by examining the crystal structures of tobermorite and jennite, the two closest crystalline analogues to the gel.

Tobermorite and jennite have three principal sites for water: (1) Water can be bound to the composite layer as hydroxyl, such as Si–OH groups in tobermorite or Ca–OH groups in jennite. (2) Water can also be bound to the composite layer as molecular water, as found in the 'pyramidal apical sites' of the Ca–O polyhedral layer of tobermorite (Merlino *et al.* 1999). (3) As mentioned above, molecular water can be associated with the Ca^{2+} ion in the interlayer space. As an illustrative example of these three sites, the structure of 1.4-nm tobermorite possesses, per formula unit, 1 molecule of water as hydroxyl (type 1), 2 molecules of molecular water associated with the composite layer (type 2), and 5 molecules of water associated with the interlayer Ca^{2+} ion (type 3). Upon dehydration of 1.4-nm tobermorite the interlayer water is easily lost at around 55 °C (Farmer 1966), leading to the 1.1-nm phase, ($Ca_5Si_6O_{17} \cdot 5H_2O$). With increasing temperature, the 1.1-nm phase persists until 250 °C, where the 0.9-nm phase ($Ca_5Si_6O_{16}(OH)_2$) forms. This phase persists until 450 °C, above which hydroxyl groups are gradually lost until wollastonite ($CaSiO_3$) is formed at 850 to 900 °C.

It is interesting that the dehydration of some forms of 1.1-nm tobermorite do not lead to shrinkage to the 0.9-nm phase. This 'anomalous' behavior (in contrast to the 'normal' behavior described above) was originally believed (Mitsuda and Taylor 1978) to be due to the presence of Si–O–Si linkages across the interlayer (i.e., double chains). However, more recent structural data indicate that this hypothesis is untenable due to the fact that all 1.1-nm phases appear to have double chains (Merlino *et al.* 1999). It has been proposed therefore that shrinkage of the 1.1-nm phase is determined by the extent to which the H-bonding network in the interlayer is disrupted upon dehydration.

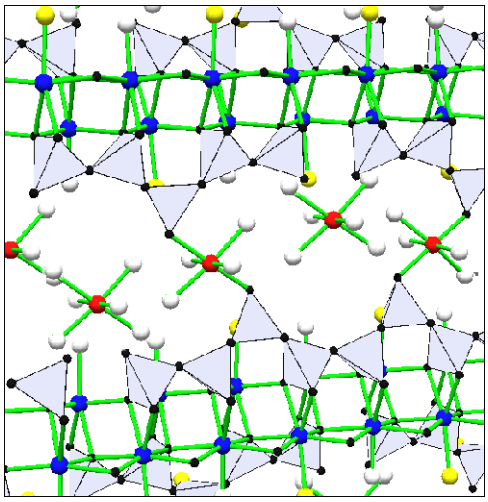

Fig. 5 Schematic representation of a possible structure for the interlayer space, which, in this example, is for an imperfect 1.4-nm tobermorite structure. Silicate tetrahedral are shown with the Ca-O sheet (blue spheres), interlayer Ca (red spheres), water molecules (white spheres), and hydroxyl groups (yellow spheres). In the figure, two "bridging" tetrahedra are replaced by an interlayer Ca ion.

The details of the water distribution in C–S–H gel are significantly less certain. Small crystal sizes, as well as defects in the crystal structure such as missing silicate tetrahedra and subsequent increases in interlayer Ca^{2+}, certainly influence the distribution of water in the interlayer space. For example, it has been argued (Chen *et al.* 2004) that, since the average Ca/Si ratio is observed to be constant with age, and since the Si–OH content is nearly zero at the high Ca/Si ratios found in cement pastes (about 1.7), an increase in the degree of silicate polymerization with age should increase the Ca–OH content in C–S–H. Further work is needed to understand the implications of this conclusion for the state of molecular water in interlayers and near surfaces, as well as on properties such as shrinkage and creep.

2.5 The Feldman-Sereda model of C–S–H

As discussed in the previous section, the structure of C-S-H at the atomic scale is similar to clays in that it is a layered structure that contains mobile and evaporable water, known as interlayer water. When water leaves the interlayer space, the layers move closer together without creating any new free surface. The behavior of this water is complicated and very important to bulk properties. Indeed, until very recently (Allen *et al.* 2007, Jennings 2008) the amount of evaporable interlayer water was uncertain. The information gained in the 1950's led to new models of the C–S–H gel phase in cement paste.

In contrast to Powers and Brownyard, who consid-

ered C-S-H to be made of colloidal-scale particles, Feldman and Sereda focused on the sheet-like structure of mineral analogues of C-S-H such as tobermorite. They advanced the alternative hypothesis that the behavior of water in the interlayer space explains many properties including drying shrinkage and creep (Feldman and Sereda 1968). In their model, gel pores as previously defined do not exist, or if they do exist they play a diminished role and do not strongly influence properties. According to their model, much of the water that adsorbs at low partial pressures is not adsorbing on a free surface but is entering interlayer spaces, and this explains the strong hysteresis in the adsorption and desorption water isotherms at pressures less than about 45% RH (see **Fig. 4**). An important implication of this hypothesis is that water vapor provides an incorrectly high surface area for cement paste.

Feldman and Sereda also argued that the small difference in molecular size between water and nitrogen could not explain the large difference in measured surface area. In their interpretation, the nitrogen molecule does not enter the interlayer spaces for energetic reasons, and thus the lower surface area value obtained with nitrogen is actually correct. The alternative interpretation proposed originally by Powers and Brownyard (1948), that the difference in surface area is because of large amount of "ink bottle" pores that allow water but not nitrogen to enter, was vigorously taken up by Brunauer (1972) who strongly argued that water is perfectly well behaved as long as the sample is prepared correctly – by D-drying and measuring the adsorption isotherm. While some efforts to resolve these points of view have been made (Taylor 1997), many details of a quantitative model remain unresolved.

Implicit in the Feldman–Sereda model is that drying shrinkage is primarily the result of water entering and leaving the interlayer spaces. Over a period of decades, much attention was paid to how the method of drying the sample before adsorption affects the measurements, and the interpretation of the resulting differences was argued openly in the literature (see for example Jennings 2008). Reversible shrinkage exhibits hysteresis on drying and rewetting, an observation that is at the center of Feldman's (1971) argument for the importance of interlayer water. Water does not easily leave and reenter the interlayer space. However, although this accounts for the observed hysteresis, changes in the amount of water in the interlayer space cause very large dimensional changes that are difficult to reconcile with observations.

The importance of this debate rests in the relative importance of surface energy, water in interlayer space, and water in the smallest pore spaces. It is widely agreed that water in the nanostructure of C-S-H controls many bulk properties including creep and shrinkage. The Powers model emphasizes the role of surface energy associated with many small pores while the Feldman–Sereda model emphasizes the importance of the disjoining pressure of water in the interlayer spaces. Neither model has been used to accurately and quantitatively relate the microstructure and nanostructure to experimental shrinkage data. Until this is accomplished, the influence of changes in formulation of cement paste on shrinkage will remain problematic.

While there are other models for gel pores, such as the Munich model (Wittmann 1979), they do not explicitly address porosity or the structure of porosity. The Munich model places emphasis on the role of disjoining pressure, which is between particles of C-S-H and not necessarily within the interlayer space. The disjoining pressure is important at higher relative humidities when multilayer adsorption occurs.

2.6 Irreversible deformation and the influence of aging

Because the models of cement paste discussed in the previous sections rest on thermodynamic considerations, they are able to address only the reversible component of shrinkage. However, cement paste undergoes significant irreversible shrinkage on drying, shown in **Fig. 4**, meaning that some of the volume change on drying is not recovered on rewetting. Cement paste also undergoes irreversible deformation on loading, known as creep. The separation of reversible and irreversible deformation is important and must be explicitly described mathematically in future models. For plastics, metals, and ceramics, creep is a thermally activated rate process, and its rate is significant only at temperatures that are greater than 50 % of the melting point or glass transition temperature. But for cement-based materials, creep is a rate process that is significant even near room temperature. Both of these irreversible deformations, shrinkage and creep, are associated with permanent structural changes to the C-S-H. Irreversible deformation is of major importance to the performance of concrete structures. Because its relative magnitude changes with time, even after the hydration reactions have become very slow or stopped, irreversible deformation must also be related to aging of cement paste.

Although the rate of creep under different conditions has been modeled extensively (see for example Bazant 2004), little has been published on the possible microstructural changes associated with either irreversible drying shrinkage or creep (Bentur *et al.* 1978). Recently, (Jennings 2008) the debate about porosity has been framed in a slightly different way by the suggestion that the C-S-H gel is granular at the nanoscale (Constantinides and Ulm 2007). One of the advantages of this approach is that rearrangement of the fundamental C-S-H particles on drying or loading provides a natural mechanism for irreversible deformation. This subject will be discussed further in Section 4.3.

An important observation regarding creep is that the creep rate decreases as the relative humidity to which the cement paste has previously been equilibrated decreases, and that there is no creep at RH values less than

50 % (Wittmann 1970). Thus, it can be concluded that either water, particularly adsorbed water on the surface of C-S-H, is necessary for creep, or that the drying shrinkage at these low RH values induces structural changes that significantly increase the resistance to creep. Furthermore, if cement paste is dried and loaded at the same time, the resulting deformation is greater than the individual contributions of creep of an undried paste (the maximum possible creep) and the deformation due to drying. The nonlinear coupling of creep and shrinkage presents a complex scenario, and at present there is no model of the nanoscale structure that can be used as a basis for quantitatively modeling these properties.

Both drying shrinkage and creep are age dependent, in that the deformation response to a given load decreases with both the degree of hydration and the degree of aging of the hydration products, principally C-S-H, after they have formed. The microstructural explanation of age as a phenomenon that incorporates both the degree of reaction and subsequent physicochemical changes within the hydration products is presently not well understood. As an example, a relatively modest increase in the curing temperature, applied for a brief period after the main early hydration period is over, significantly reduces the subsequent irreversible drying shrinkage (Thomas and Jennings 2002) by an amount that is far out of proportion to any increase in the degree of hydration.

Some mathematical models of shrinkage and creep, like that of Bazant *et al.* (2004) incorporate aging to account for long term shrinkage and creep over a wide variety of environmental conditions. A few theories of aging have been advanced, and these generally rely on the observation that the degree of polymerization of C-S-H continues to increase over time after it forms, making it stiffer. This does not seem to present a complete solution, however, as there are some aspects of creep and shrinkage, such as their sensitivity to the rate of change of temperature or relative humidity, that are difficult to relate to the degree of C-S-H polymerization. In future research, it will be necessary to develop a theory of aging that is based on nanostructural changes to the C-S-H gel. At present, there are no known relationships between aging and porosity, although one study (Bentur *et al.* 1978) reported some interesting changes in the pore structure of C_3S paste resulting from drying and loading.

3. Evolution of the pore system with time – rate of reaction and capillary pores

Cement based materials develop structure and gain strength as a result of chemical reactions between cement and water that form several different hydration products. As noted previously, as hydration proceeds the volume of gel pores increases while the volume of capillary pores decreases. From an engineering point of view, the rate at which Portland cement hardens, or gains strength, which is directly related to the rate of formation of the hydration product, is an important characteristic that determines the amount of time available for mixing and placing of concrete, and the curing time required for the concrete to reach a minimum strength so that construction can continue. From a scientific point of view, microstructural evolution rates, and the final microstructure of the material, are determined by the kinetics of the set of coupled chemical reactions that occur. It may therefore be anticipated that comprehensive, fundamental models of concrete will predict properties and performance by first simulating the formation of the microstructure and nanostructure of the cement paste, and then calculating properties based on this simulated material. There have been recent advances in understanding the theoretical basis for the measured hydration kinetics of cement, which are reviewed in this section.

3.1 Overview of cement hydration kinetics

Under normal conditions, for the first few hours after mixing, concrete is fluid and workable and can be placed into forms. It then gains strength rapidly, attaining a significant fraction of its final strength after just 24 h. For construction purposes, this is much more useful than would be a linear or declining rate of strength gain throughout the first 24 h. One of the oldest discussions in the literature concerns the mechanisms that control the reactions (Gartner and Gaidis 1999) and therefore determine the kinetics.

The rate of reaction of a typical ASTM Type I ordinary Portland cement (OPC), as measured by isothermal calorimetry, is shown in **Fig. 6**. With this method, the progress of the chemical reactions between the cement and water is monitored by measuring the exothermic heat produced. Just after mixing, a significant burst of heat is measured (region 1 in **Fig. 6)**, corresponding to

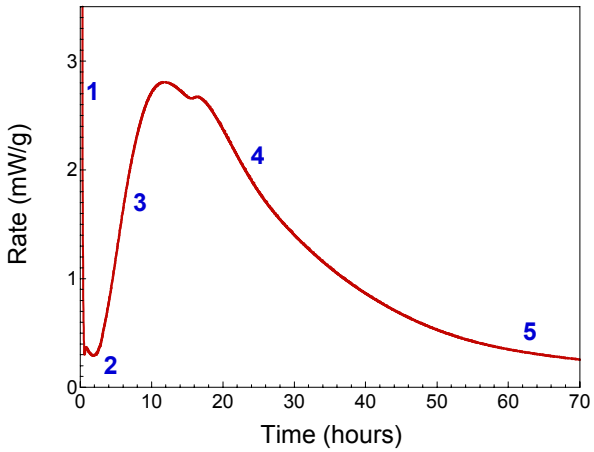

Fig. 6 Rate of hydration of a typical Portland cement, as measured by isothermal calorimetry at 20˚C. The five kinetic regimes are discussed in the text.

wetting of the cement particles and rapid dissolution of a small amount of the cement minerals, particularly the calcium aluminates and the alkali sulfates. The rate of heat output declines rapidly and then remains rather low for a period of a few hours (region 2), during which time the paste remains in a relatively plastic, fluid state and can be pumped, placed, and finished. During this induction (or dormant) period, hydration of the calcium silicate minerals to form the main hydration product, C-S-H gel, is quite slow. When the hydration rate increases again after a few hours, it is dominated by the hydration of C_3S to form C-S-H and calcium hydroxide (CH). The kinetics of this reaction are governed by nucleation of hydration product near the surface of the cement minerals and growth of these product regions into the water-filled capillary space between the particles.

The shape of the main hydration rate peak is characteristic of a nucleation and growth transformation. The total rate of hydration is determined by the rate at which dissolved ions precipitate out of the solution to join the solid hydration products. This rate is proportional to the amount of interface between the new phase (hydration product, primarily C-S-H) and the old phase (pore fluid) at a given time. Initially, the interfacial area increases as regions of hydration product increase in size and new regions form (region 3), while at later times the interfacial area decreases as adjacent regions come into contact (region 4). The impingement, or intergrowth, of hydration product regions from different cement grains is what causes cement paste to set and then gain strength. This process also determines the complex distribution of capillary and gel porosity in the hardened paste. A mathematical model of this process is discussed in the next section.

After the cement grains are covered with a continuous layer of hydration product (region 5), the rate at which ions can diffuse outward from the unhydrated cement particles to the remaining capillary pore space becomes rate limiting. During this final diffusion-controlled kinetic regime (see **Fig. 6**), the hydration rate declines slowly for weeks, months, or even years, depending on factors such as the cement particle size distribution, the mix design, and the curing conditions. Over this time scale, the slow but steady hydration of C_2S makes a significant contribution to the strength.

3.2 Hydration kinetics of C_3S – mathematical models

The hydration kinetics of pure C_3S are broadly similar to those of OPC, since C_3S hydration dominates the early hardening of OPC cements. C_3S hydration is therefore widely studied as a simple, but highly relevant, model system for OPC. The early hydration kinetics of C_3S have frequently been interpreted by fitting a standard Avrami-type equation for transformation by nucleation and growth to experimental data (Thomas and Jennings 1999). The Avrami equation provides reasonable fits to most of the main hydration rate peak measured by calorimetry, but the resulting parameters are difficult to interpret (see discussion in Thomas (2007)). This is because the Avrami equation assumes spatially random nucleation throughout the transforming volume, whereas it is well established that for C_3S and Portland cement, the hydration product nucleates only on or near the surface of the particles (Taylor 1997).

Thomas (2007) recently proposed an alternative set of nucleation and growth equations for interpreting C_3S hydration kinetics:

$$X = 1 - \exp\left[-2O_v^B \int_0^{Gt} \left(1 - \exp\left(-Y^e\right)\right) dy\right]$$

$$Y^e = \frac{\pi I_B}{3} G^2 t^3 \left[1 - \frac{3y^2}{G^2 t^2} + \frac{2y^3}{G^3 t^3}\right] \quad (\text{if } t > y/G) \qquad (6)$$

$$Y^e = 0 \quad (\text{if } t < y/G)$$

where X is the fraction transformed at time t, O_v^B is the amount of C_3S surface area per unit volume on which nucleation can occur, I_B is the intrinsic rate of nucleation per unit area of C_3S surface, and G is the linear growth rate of hydration product in any direction. Equation (6), which in its original form was used to describe a solid state transformation nucleated preferentially on internal grain boundaries (Cahn 1956), provides a physically realistic basis for modeling the early hydration of C_3S and, consequently, gives better fits to the kinetic data.

In Eq. (6), note that y and Y^e are temporary constants that disappear upon integration, so the transformation rate $X(t)$ depends only on the three fundamental physical parameters O_v^B, I_B and G. Of these, the boundary area O_v^B can be determined independently from the surface area of the starting powders. **Figure 7** shows isothermal

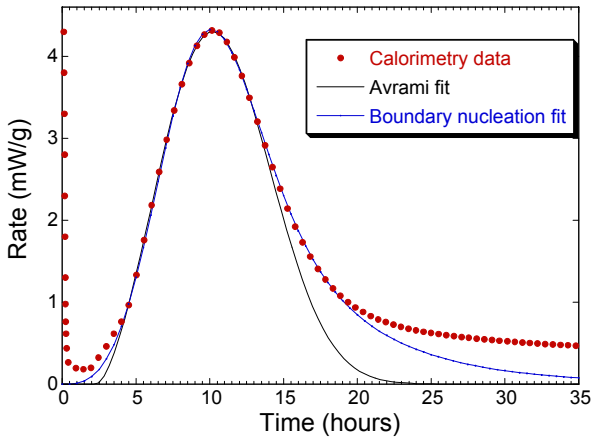

Fig. 7 Rate of heat evolution from a C_3S paste mixed at a water/cement ratio of 0.5 by mass and hydrated at 20°C (solid circles), after Thomas (2007). Fits obtained by applying the standard Avrami nucleation and growth equation and the boundary nucleation and growth model (Eq. 8) are shown.

calorimetry data for a C_3S paste, along with fits to the data made both with the Avrami equation and with the surface nucleation model, Eq. (6). Despite having one fewer fitting parameter, the surface nucleation model provides a significantly better fit to the main hydration peak, indicating that it also provides a better physical description of the early hydration process.

3.3 Changes to the pore system with age

For the present paper it is relevant to ask how the early hydration kinetics can be related to, or made consistent with, the resulting microstructure. In particular, it is becoming increasingly clear that the C-S-H gel phase is "nanogranular" (Bentz *et al.* 1995, Constantinides and Ulm 2007), that is, made up of discrete nanometer-scale solid particles that are agglomerated into random clusters separated by water-filled spaces that constitute the gel pores. The limited size to which the C-S-H particles grow seems in a sense to contradict the nucleation and growth models, which dictate that the individual regions of hydration product grow until they contact adjacent similar regions. However, these observations can be reconciled by proposing that the growth of C-S-H is autocatalytic (Gartner and Gaidis 1989, Thomas *et al*. 2007b), such that C-S-H particles tend to form in contact with existing particles. Growth of hydration product thus occurs by the continued local nucleation and limited growth of these nanoparticles of C-S-H. A significant issue for future research is to understand what controls the packing arrangement of the particles. These processes can be simulated giving results as shown in **Fig. 8**, and therefore these algorithms can be tested against detailed measurements of the C-S-H structure.

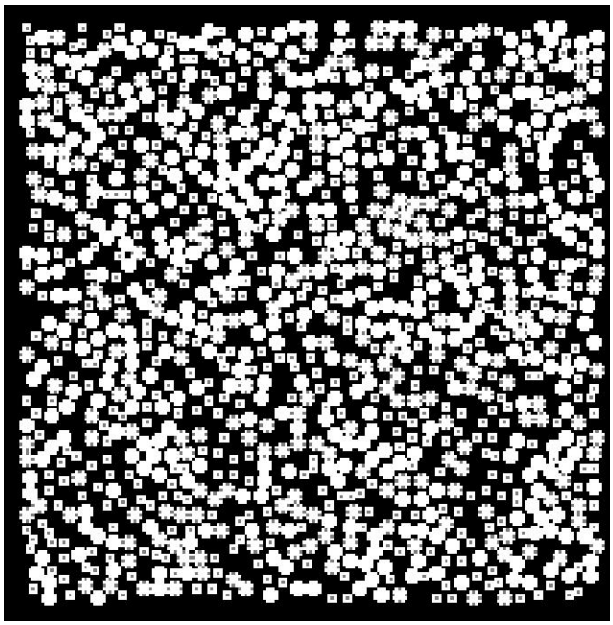

Fig. 8 Example of a simulated nanogranular structure obtained from a simple digital model. The structure is seeded with a single particle at the center of the box, and then new particles form randomly in contact with existing particles as long as space is available. The simulation is continued until particles reach the edge of the box. This type of process is compatible with the observation that the hydration kinetics are controlled by nucleation and growth of hydration product (see Sections 3.1 - 3.2), and with the nanogranular structure of the C-S-H phase inferred from nanoindentation measurements. The average packing density and the distribution of interparticle porosity both depend on the specific rules governing the formation of new particles and the ability of particles to rearrange after they form.

4 Recent advances in characterizing C-S-H structure

Over a period of decades, the size distribution of the smallest pores in cement paste has been investigated extensively. These pores are abundant and have reasonably distinct sizes. Gas sorption using nitrogen and other adsorbate gases has been used extensively to measure surface area and pore size, mercury intrusion has been used to measure pore size distribution, and techniques like NMR and small angle neutron scattering have made recent contributions, as is discussed further below. A summary of the gel pore size and the techniques used to measure it is included in **Table 1**, based on a recent model (Jennings 2004).

High resolution microscopic techniques have provided a significant amount of qualitative information about the structure of C-S-H, although of necessity in its dried state due to the requirement for high vacuum. Increasing evidence points to the gel being composed of tiny particles with a brick like shape (Richardson 2002). These particles have dimension of a few nanometers in cross section and 10 nm or greater in the long direction. This picture is derived from both transmission electron microscopy (TEM) and atomic force microscopy (AFM) (Nonat 2004) evidence. TEM micrographs have been obtained from C-S-H as it has formed in paste, and these images broadly reinforce the longstanding hypothesis that C-S-H forms with two different structures. These structures have been called inner and outer product, middle and late product (Jennings *et al.* 1981), phenograins and groundmass (Diamond and Bonen 1993), and most recently high density and low density C-S-H (Tennis and Jennings 2000, Jennings 2000). A problem with TEM, gas sorption, and other techniques is that the pore structure is altered by the drying treatment in ways that are not fully understood. Indeed, the gel porosity, which is a dominant feature at the nanometer scale, is not particularly evident in TEM micrographs.

Two modern techniques that can provide information about the nanostructure of C-S-H without drying are small-angle scattering and NMR, and the recent contributions of these techniques are discussed in the next two sections. It should be noted that to date only limited attention has been paid to the structural changes that

Table 1 Predictions of colloid model and measured values for various properties of C-S-H, after data in Jennings (2004).

Name of unit in structure	Radius[a] of unit (nm)	Computed density[b] (kg m^{-3})		Measured density (kg m^{-3})	Specific Surface area (m^2 / g of C-S-H)	Model porosity[c] (%)	Porosity based on composition[d] (%)	Measured composition (RH of measurement)	Pore radius (nm)		
		Pores empty	Pores full						Model	Experiment	
Basic Building Block	1.1	2800	2800	2800	1000[f]	-	0 no H_2O	1.7 $CaO•SiO_2•$ 1.4 H_2O (Dry – no H_2O)	-		
Globules	2.8	2300	2480	2450	460[g]	18	16 vol % .7 H_2O	1.7 $CaO•SiO_2•$ 2.1 H_2O (11%, .7 H_2O)	0.24-0.45 0.24-0.45	17 5	
LD	8.3	1440[e]	1930		250[e]	49 37%*	*Random Jammed*		1.2-1.3		
Average[h]			2030	2000		43.5	42 vol % 2.6 H_2O	1.7 $CaO•SiO_2•$ 4.0 H_2O (Saturated, 2.6 H_2O)			
HD	>100	1750[e]	2130		0	38 24%*	*Close Packed*		1		
Inter LD									2 10-15	0.5-5	2.5 10

[a]Assuming spherical particles; using relation r = 3/(SSA * ρ) where r = radius, SSA= specific surface area, and ρ = density
[b]Based on volume fraction of solid and pores
[c]Calculated as $(1 - \rho_{unit}/\rho_{basic\ building\ block}) * 100$.
[d]Computed from the molar volume of dry C-S-H and the molar volume of water. The molar volume of dry C-S-H ($1.7CaO·SiO_2·1.4H_2O$) was computed by dividing the molecular weight by the measured density to obtain a value of 6.45×10^{-5} m^3/mol.
[e]Values were optimized by maximizing the statistical fit between reported values of nitrogen surface areas, pore volumes, and capillary porosity with predicted values of the model.
[f]Based on SAXS data.
[g]Based on SANS data, assuming that only the LD C-S-H structure contributes to the surface area.
[h]Assuming 50 % LD (10) for w/c = 0.5.
*Excluding porosity in globules.

occur as a result of drying or applied load, and in general little has been learned about the changes that occur due to aging. With new information comes new insight, and more research in this area should be profitable.

4.1 Small-angle scattering techniques

Small-angle scattering (SAS) using neutrons (SANS) or X-rays (SAXS) is a powerful method of characterizing the micro- and nanostructures of disordered heterogeneous materials, and the technique can be used to study wet samples. It is of particular interest for materials that are amorphous over length scales short enough such that diffraction techniques are ineffective, as is the case for the C-S-H gel phase of cement paste. Another important advantage of SAS for cement paste is that specimens can be analyzed in their natural saturated state, without any drying or other pretreatment that can affect the delicate nanostructure. For these reasons, SAS has been increasingly applied to hydrating cement systems in recent years, providing a significant amount of new information (Allen and Thomas 2007).

The angular profile of the SAS intensity is effectively a Fourier transform of the microstructure that generates it, and can in principle be analyzed to determine the size distribution, volume fraction, and shape of the scattering features. For complex microstructures such as that of cement paste, the data are interpreted using microstructural models that generate quantitative parameters. For example, the Porod scattering relationship can be used to measure the total internal surface area of the scattering phase per unit volume of specimen. This specific surface area is a useful indication of the total active interface between the hydration product and the pore system. Recent SAS measurements of the specific surface area of cement indicate values ranging from 100 m^2/cm^3 to 150 m^2/cm^3, or about 70 m^2/g to 100 m^2/g of dry paste (Thomas and Jennings 1999, Jennings 2008, Allen and Thomas 2007). The surface area increases slightly with long-time curing, and is greater when the w/c of the paste is higher.

A more comprehensive microstructural model incorporating surface-fractal and mass-fractal components

has been used to model the scattering from a wide range of length scales (Allen 1991). This model is based on fundamental building-block particles of C-S-H gel that are randomly packed into relatively low-density structures that comprise the outer hydration product in the capillary space of cement paste. The size of the fundamental particles is 4 nm to 5 nm, and the similarly-sized spaces between the packed particles comprise the gel porosity. It should be noted that the type of fractal scaling observed from normal cement systems is quantitatively different from what would be generated by a layered or sheet-like morphology, indicating that the sheet-like chemical structure of the C-S-H gel does not extend to length scales above that of the fundamental particles (e.g., 5 nm).

An important issue in understanding and modeling the C-S-H gel phase in cement paste is determining the role of water in pores of various sizes. While it is clear that water in the larger capillary pores will behave essentially like liquid (bulk) water, and that OH groups in the C-S-H and CH will be part of the solid phases, there is significant ambiguity regarding water in gel pores with sizes of the order of 1 nm. Recent SAS measurements exploiting the different scattering properties of hydrogen and deuterium have established the molar composition (1.7C-S-1.8H) and mass density (2.60 g/cm^3) of the solid C-S-H phase in contact with the pore system (Allen *et al.* 2007). This provides an important baseline value for modeling efforts.

Because SANS is conducted on saturated specimens, the microstructural changes associated with drying can be investigated by comparing the SANS response of the same paste before drying and then after drying and resaturating. A recent investigation of this type (Thomas *et al*. 2007) found that at RH levels above 50 %, capillary stresses compact the C-S-H gel and increase its density. Drying and resaturating also reduced the surface area, particularly at RH levels below 50 %. This was attributed to a loss of surface area at C-S-H particle contacts as the average interparticle spacing decreased.

Another recent SANS investigation (Jennings *et al*. 2007) found that a short period of elevated temperature curing caused the local packing density of the C-S-H gel to increase and the surface area to decrease, an effect quite similar to that of drying. In addition, extended curing at 20˚C had a similar effect. These results suggest that aging of cement paste resulting from different causes such as time, heating, and drying, are all related to changes in the orientation and packing of the C-S-H nanoparticles.

4.2 Nuclear magnetic resonance

Nuclear magnetic resonance (NMR) analysis, which is used to study a wide variety of atomic-scale interactions in materials, is an extremely useful technique for application to cement chemistry. In particular, as with SANS, NMR can be used to study wet samples. The technique is based on the fact that most atomic nuclei have a non-zero spin state. The rate at which the spins align themselves with a static magnetic field (spin-lattice NMR), or the response of the material to an oscillating magnetic field (spin-spin NMR), provides information about atomic interactions with adjacent nuclei and with the surrounding medium. The most widely used NMR application to cement is ^{29}Si NMR, which allows the bonding state of the silicates in the hydration product to be monitored. NMR enables the average chain length of the silicate backbone in the C-S-H gel to be measured, a parameter which shows significant variation depending on composition and curing conditions.

Another NMR application with particular relevance to the pore system in hydrated cement is ^{1}H relaxation. The relaxation times of hydrogen nuclei within water molecules are determined by the chemical and physical environment of the water, and measurement of these relaxation times provides information about the pore system. Two relaxation times are generally measured: T_1 is the spin-lattice relaxation time, and T_2 is the spin-spin relaxation time. In general, diffusing protons are able to relax when they encounter a pore surface. If the diffusion rate is fast compared to the surface relaxation rate, then a single averaged relaxation rate is observed which is proportional to the pore surface/volume ratio.

Halperin *et al*. (1994) derived an expression for the total surface area accessed by mobile water in a specimen based on the measured T_2 relaxation time, and they were able to observe the development of the surface area during the hydration of a white cement paste. They found that the surface area increased rapidly between 6 h and about 48 h, and that there was little surface area increase between 100 h and 1000 h. Similar behavior was previously observed when the surface area was measured with SANS (Thomas *et al*.1998). This clearly indicates that the surface area of cement paste is associated with the porous hydration product that forms rapidly in the capillary pore system during the early nucleation and growth period of the hydration process. The maximum surface area measured by NMR is about 280 m^2/g dry paste, which is considerably higher than SANS values. It is generally observed that different techniques measure very different surface areas for cement paste (Thomas and Jennings 1999), a discrepancy that can be generally attributed to the complex morphology across many length scales of the C-S-H gel phase.

Quite recently, two-dimensional T_1 –T_2 correlation experiments have provided direct information on the pore size distribution and have established that water exchanges readily between the gel and capillary pore networks (McDonald *et al.* 2005, 2007; Monteilhet *et al.* 2006). In addition, these experiments suggested that the gel and capillary pore system were clustered in two ranges with sizes of 0.9 nm to 1.4 nm and 7 nm to 30 nm. This observation was further refined by NMR dispersion measurements (Korb *et al.* 2007) that found four discrete pore diameter ranges with average values of 1.8 nm, 7 nm, 50 nm, and 600 nm. This provides consider-

able support to the view that the C-S-H gel consists of solid particles of a characteristic size on the order of 5 nm. In particular, similar pore sizes were proposed previously by Jennings (2000) as part of a quantitative colloid model of C-S-H gel.

4.3 Colloid model of C-S-H

During the past decade, attempts to combine the results of multiple experimental techniques (Jennings and Tennis 1994, Tennis and Jennings 2000, Jennings 2004, Jennings *et al*. 2007) has resulted in the development of a colloid model now referred to as CMII (Jennings 2008). A cartoon of the proposed structure is shown in **Fig. 9**. The model is granular, with each grain (Little brick) being about 4 nm to 5 nm across, and a few layers thick. Each grain contains both interlayer water that results in volume change as water comes and goes, and very small pores, 1 nm to 4 nm, that can empty without changing the volume of the particle.

This model describes the low density (LD) C-S-H, which forms primarily during the nucleation and growth period. The nanostructure is granular, and sliding at particle contacts provides a mechanism for irreversible deformation for this nearly brittle material. Particles reorient and slide over each other with time, the application of load, or by drying. Some of the predictions of this model are included in **Table 1**. The advantages of this granular model include a physical explanation for deformation and a quantitative description of water in the smallest pores, including the so called constrained water. Viscous flow does not change the specific surface area except for the small amount caused by bringing particles closer together. Also, the very large local deformations observed on drying (Neubauer and Jennings 2000) are explained, along with the observed distribution of Young's modulus values measured by nanoindentation (Constantinides and Ulm 2004, Jennings *et al*. 2007). Further research will lead to other implications of the granular approach and its consequences for bulk properties. It is important to note that seemingly contradictory results from several experimental techniques have been reconciled using the granular model in its present form, and this is one of the most important contributions a model can make to scientific understanding.

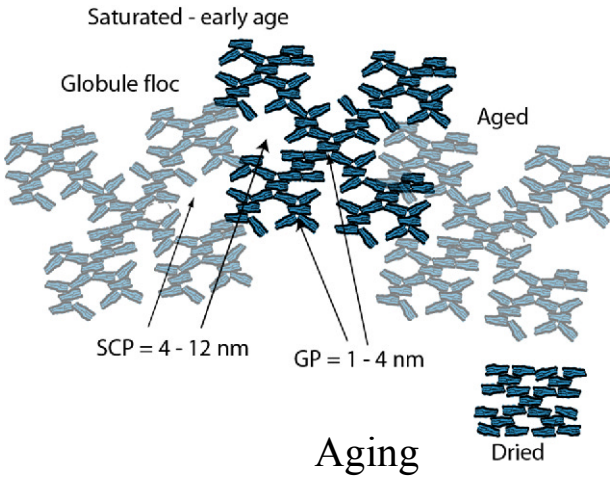

Fig. 9 Schematic of particles of C-S-H, referred to as globules or bricks. They are about 4 nm across and have a layered structure with interlayer space and small pores where the layers imperfectly align. Their packing arrangement is such that the pores tend to have specific sizes and overall packing efficiency. These characteristics are outlined in Table 1. SCP are small capillary pores and GP or gel pores.

5. Application of computer modeling to cement research

5.1 Overview

The foregoing discussion has made clear the enormous complexity of cementitious materials, which makes it difficult to characterize them and to predict their performance. There are many interrelated phenomena, some of which are well understood and others for which our knowledge is incomplete and inadequate. Structure-property models have become computer intensive. This section describes how progress can be made on these issues through the application of digital and mathematical models, using high-performance computers as another kind of experimental tool.

The use of computational models for materials research involves an intimate interaction with "traditional" experiments. For one thing, a fundamental model of a material system must be endowed with the best available knowledge of the physics or chemistry pertinent to the material, and this knowledge must have its source in experimental observation and analysis. On the other hand, as we have shown, there are instances where experimental observations appear to conflict with each other or lead to different theories about the processing-structure-property relationships that we wish to understand and quantify. In these instances, fundamental computer models can be used to test different theories or even to test new ideas that might bring a wider range of observations into harmony but which are too complex to investigate without the aid of a high-performance computer.

Generally, models of structure-property relationships attempt to calculate some property of the material based on structure, which is assumed *not* to be changing, at one or more length scales. These models may be divided into two types: 1) Models that explicitly require information about the geometric distribution of phases and pores. These models are generally computer intensive 3-D representations of the structure at some length scale. 2) Models that average the microstructure into a homogenized volume and predict a property independent of the geometric distribution of phases and pores. The properties of individual phases and the volume fraction of each phase serve as a starting point. At a given scale, two or more phases are homogenized into one effective phase over a significantly larger scale. The process may

be repeated up to the scales of importance to engineering properties.

5.2 Geometric models of hydration and microstructure

Geometric models for calculating a composite material property rely on the assumption that two types of information are necessary and sufficient: (1) the values of the property for each of the individual constituents of the composite and (2) the volumes and 3-D arrangement of each of those constituents. For example, to calculate the Young's modulus of a hardened cement paste, a geometric model, such as the linear elastic finite element model for digital images developed at NIST (Haecker *et al*. 2005) requires the input of the linear elastic moduli of each phase that is present in the material, including the porosity, and a 3-D digital representation of the cement paste microstructure with a resolution of 1 μm. As another example, to calculate the permeability of pervious concrete, a geometric model like the Stokes Permeability Solver developed at NIST (Bentz 2007) requires a digital image representation of the 3-D structure of the concrete at millimeter resolution, and the assumption that solid regions have zero permeability.

The detailed distribution of phases, which we collectively call *microstructure*, is often difficult to obtain because it involves a specification of the phase that is present at each point (*x,y,z*) in space. A few experimental techniques, such as X-ray computed microtomography (Kak and Slaney 2001, Bentz *et al*. 2002) and focused ion beam nanotomography (Holzer *et al*. 2006) are capable of finely resolving the 3-D pore/solid structure of cement paste at a given age of hydration, although a separate technique would be required to segment the solid phases. In this connection, a reliable and fundamental model of the kinetics of microstructure changes, such as HydratiCA (Bullard 2007b), can be useful for predicting the microstructure as a function of time, providing snapshots of the structure at any given time that can be used as input to a structure-property model. Thus, first we review microstructure.

Several notable attempts have been made to simulate the kinetics of microstructure evolution in cement paste, including the early work of Jennings and Johnson (1986), the HYMOSTRUC model developed at TU Delft (Breugel 1991), and the CEMHYD3D model developed at NIST (Bentz 1997). These models have been successful at predicting properties of cement paste that depend on the capillary pore system. The primary limitation of these models, however, has been that they model the kinetics of microstructure development using semi-empirical parameters that must be calibrated to experimental results for any given cement formulation or mix design.

5.3 Hydration modeling based on fundamental chemical principles

It would be preferable to model the kinetics according to the individual fundamental chemical reactions that occur during hydration, according to accepted principles of chemical kinetics and transition state theory. The necessary kinetic parameters of each reaction could be measured in a laboratory once for each mineral of a given composition—admittedly a challenging task—and then used to model any cement mix design equally well without further calibration. This latter approach has been adopted recently to develop a new microstructure model called HydratiCA (Bullard 2007b). It is based on the recognition that there are only four primary rate processes that govern structural changes in cement paste: (1) dissolution and growth of mineral phases, (2) diffusion of mobile species in solution, (3) complexation reactions among species in solution or at solid surfaces, and (4) nucleation of new phases. The kinetics of all four of these basic processes are unified by the principles of transition state theory (TST) (Glasstone *et al*. 1941, Darken and Gurry 1953).

According to TST, any observable rate process can be described in terms of a free energy surface. If the entropy of activation is assumed independent of temperature, then the rate constants for a reaction in the forward and reverse directions are

$$\begin{aligned} k_+(T) &= k_+(T_0)\exp\left[\frac{-\Delta H_+^*}{k_B}\left(\frac{1}{T}-\frac{1}{T_0}\right)\right] \\ k_-(T) &= k_-(T_0)\exp\left[\frac{-\Delta H_-^*}{k_B}\left(\frac{1}{T}-\frac{1}{T_0}\right)\right] \\ &= k_-(T_0)\exp\left[\frac{-(\Delta H_+^* + \Delta H_{rx})}{k_B}\left(\frac{1}{T}-\frac{1}{T_0}\right)\right] \end{aligned} \tag{7}$$

where T_0 is a reference temperature at which the values of the rate constants are known, ΔH_+^* and ΔH_-^* are the activation enthalpies for the forward and reverse processes, respectively, and ΔH_{rx} is the enthalpy of reaction. It is important to recognize that the rate constants in Eq. (7) are absolute rate constants for the elementary reaction in question, not the net rate constant that would be readily measured in a laboratory. The latter quantity will depend on the instantaneous quantity of reactants and how far the reaction is from equilibrium when the measurement is made. However, by keeping track of both the forward and reverse rates for a given elementary reaction using Eqs. (7), one can simulate the net rate of the reaction, regardless of the concentrations of each substance at any particular moment. In particular, if the reaction is at equilibrium then the forward and reverse rates must be equal, which implies that their ratio equals the equilibrium constant for the reaction. In this way, TST provides an explicit link between the rates of reaction (chemical kinetics) and the equilibrium state (thermodynamics). Furthermore, because k_+ and k_- depend on temperature according to Eq. (7), this approach provides the dynamic basis for the temperature dependence of the equilibrium constant, known as the van't

Hoff relation (van't Hoff 1903). Thus, a complete dynamic description of local kinetics and equilibria over a modest temperature range is given by values for k_+ and k_- at a reference temperature (or only one rate constant when K_{eq} is known), together with the activation enthalpy in either direction and the net enthalpy of the reaction.

The details of how these kinetic principles are incorporated and tied to microstructure development do not fit within the scope of this paper, but the reader may obtain a complete description in other papers (Bullard 2007a, 2007b). In brief, a cubic 3-D lattice is defined with spacing λ between lattice sites. The initial cement paste microstructure is mapped onto this lattice by assigning a phase (e.g. alite, aluminate, gypsum, water) to each lattice site. These materials are themselves finely discretized into small quanta of concentration called cells; the number of these cells of a given material at a particular lattice point determines its concentration there, and multiple materials may be present at a given lattice point.

Figure 10 shows a flow chart of how HydratiCA simulates microstructure evolution (this flow chart is qualitatively reminiscent of that used for the Jennings model of microstructure (Jennings and Johnson 1986)). In HydratiCA, transport of mobile species is simulated by allowing each cell at a lattice site to execute a random walk to a neighboring site, the probability of the walk depending on the intrinsic mobility of the cell at the site and the length of the time increment being considered. The probabilistic rules are formulated to accurately reproduce the kinetic laws of diffusion or advection (Bullard 2007a). Similarly, any given chemical reaction at a lattice site is simulated by a probabilistic rule, in which the probability of the reaction occurring depends on the reaction rate constant and on the numbers of cells of each reactant that participates in the reaction (Bullard 2007b). The microstructure evolves automatically as the model updates the types and numbers of cells at each lattice point in the system for a small time increment, and then the whole cycle is repeatedly executed to simulate longer times (**Fig. 11**).

This modeling procedure is quite general and can accommodate a wide range of coupled reaction and transport phenomena if the model is given the correct kind of input. This input includes the necessary information for each fundamental reaction that can occur (rate constant, activation energy, nucleation energy barriers, and stoichiometry) as well as the intrinsic mobilities of each diffusing solute species. In addition to the reaction parameters, several properties of each of the constituent substances are also required. For simple condensed phases, the density (ρ), molar volume (V_m), and, for adiabatic simulations, the isobaric heat capacity (C_p) must be supplied. For mobile solute species, one must supply the electrical charge (z), the diffusion coefficient at infinite dilution (D_0) and ion-specific parameters necessary to calculate the activity coefficients (Harned and

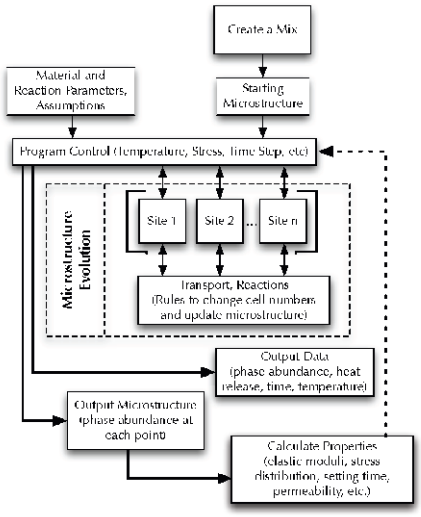

Fig. 10 Flow chart illustrating the algorithms, program control, and data flow of the HydratiCA model of hydration.

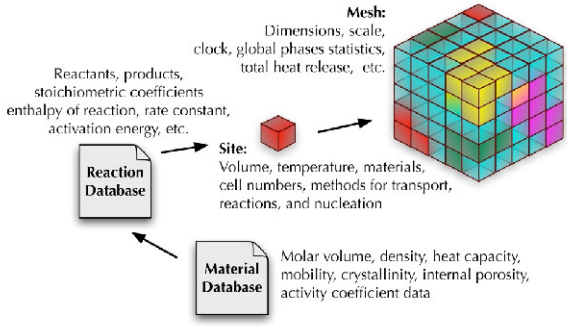

Fig. 11 Data structures and relations in the HydratiCA model of hydration.

Owen 1958). Values for many of these properties can be found in textbooks or other reference materials (Taylor 1997, Mills and Lobo 1989). For solids that can exhibit a range of chemical compositions (such as C-S-H), the model handles the compositional variability by a solid solution approximation using stoichiometric end members to encompass the range of compositions. Each end member is assigned values for all the properties just enumerated, and then the relative rates of formation of each member at a lattice site determine the local composition of the phase.

Although a number of fundamental parameters are required for input, there is no explicit dependence on mix design or cement clinker composition. In other words, one of the powerful motivations for developing this kind of model is that one does not need to adjust any of the reaction parameters to simulate different mixes. Instead, the differences between mixes, such as water-solids ratio, clinker composition, and particle size distribution, are specified at the beginning of the simulation through the assignment of the cell types and numbers at each lattice point.

This paper has detailed some of the important structural information that is encoded over a range of length scales, and this multiscale structure must be accommodated in a model like HydratiCA because the structure at each length scale can have important consequences for kinetics. **Figure 12** shows a hypothetical nanoporous material that is composed of solid building blocks (the gray circles) aggregated in a random fashion. When the lattice is fine enough that the individual details of the structure can be discerned, as in (A), then one can consider this nanoporous structure as a two-phase material and can proceed as already described. However, if the lattice is much coarser, as in (B), then the details of the structure are mostly lost. In this latter case, one must assign "effective" properties to the material. These include not only effective values for the density and molar volume, but also an effective porosity, surface area, and tortuosity of the pore structure. Clearly, the former approach with finer lattice spacing is preferable for simulating the growth and structure of such phases. However, in many circumstances the goal of a microstructure model is to track the structural evolution at length scales of ≥ 100 μm, making nanoscale lattices unfeasible from a computational standpoint.

There are two important ways that a model like HydratiCA can be used to advance cement science. First, it can be used as a research tool for investigating mechanisms of hydration and degradation of cement paste, and secondly it can be used to produce snapshots of the 3-D microstructure at any instant in time, with which engineering properties may be calculated, as detailed earlier in the paper.

We give here one example where this modeling approach has been used to shed light on the mechanism by which the pore system evolves in cement paste, using tricalcium silicate (C_3S) as an idealized model (Bullard 2008). There is some controversy over the nature of the induction period in the early stages of C_3S hydration. According to one leading theory, which we call the metastable barrier layer (MBL) theory, a thermodynamically metastable hydrate phase (C-S-H(m)) forms on the surface of cement particles within seconds of wetting (Stein and Stevels 1964, Gartner and Gaidis 1989). This hydrate is assumed to approach equilibrium with the surrounding solution and also acts as a protective barrier against further dissolution. This qualitatively explains two important experimental facts about the induction period: (1) that hydration rates are very low, and (2) that the solution chemistry changes very slowly. According to this theory, the acceleration period begins when a more thermodynamically stable hydrate phase (C-S-H(s)) nucleates and grows at the expense of the metastable form. The C-S-H(s) phase is assumed to be more permeable than C-S-H(m), so the gradual disappearance of the latter phase, combined with the ever increasing surface area of the growing C-S-H(s) phase, corresponds to ever increasing rates of hydration.

An alternative theory has been developed to explain

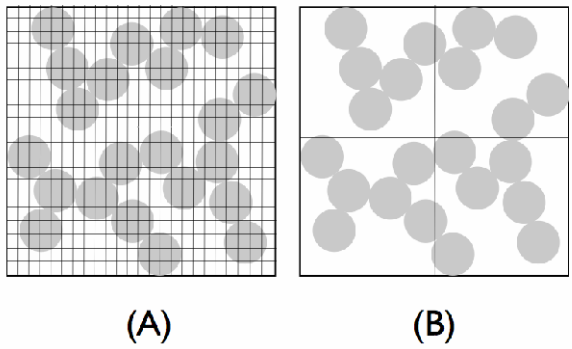

Fig. 12 Hypothetical nanostructured material consisting of randomly aggregated solid particles (gray circles) surrounded by porosity, showing the importance of model scale on the strategy for simulation. If the model lattice spacing is very fine (A) then the nanopore structure can be resolved and transport and reactions can be simulated explicitly. If the lattice spacing is coarse (B), then the solid material at each site must be assigned an effective internal porosity, surface area, and tortuosity to properly simulate the material's resistance to solute transport.

the kinetics of early-age hydration. In this theory, (stable) C-S-H nucleates on the surface of cement grains within minutes of wetting, due to its very low solubility. The rates of formation of C-S-H are initially very low at first because of the small surface area of the stable nuclei. At the same time, the rate of dissolution of cement grains is inhibited by poisoning of the active dissolution sites by adsorption of calcium or hydroxyl ions from the solution (Damidot *et al*. 2007). The observed slow changes in solution composition are assumed to be the result of a steady state condition, as opposed to a near-equilibrium state, in which the rate of dissolution of cement is nearly equal to the rate of growth of C-S-H. By this latter theory, which will hereafter be called the steady-state theory, the ever-increasing surface area of C-S-H as it grows is responsible for the ever-increasing rates of hydration, i.e. C-S-H growth is assumed to be rate-controlling. This assumption has been used to develop models that provide a good fit to experimental data on hydration of C_3S and C_2S at intermediate ages (Garrault and Nonat 2001), and it also is a basic assumption of the new mathematical boundary nucleation and growth model of C_3S hydration kinetics (Thomas 2007) described in Section 3.2.

HydratiCA has been used to test each of these two theories. To investigate the MBL theory, metastable and stable forms of C-S-H were defined in terms of their compositions, molar volumes, densities, transport factors, and reaction rate constants, listed in **Table 2**. Because the forward and reverse rate processes are simulated at a local level, the approach to equilibrium between C-S-H and the solution happens naturally. Similarly, the proposed phase transformation between

Table 2 Material properties and reaction rate constants used in HydratiCA to model hydration of C_3S, after Bullard (2008).

Material/Ion	Formula	ρ (kg/m^3)	V_m (10^{-6} m^3/mol)	Transport Factor	D_o (10^{-9} m^2/s)	k_{diss} (10^{-6} $mol/(m^2 \cdot s)$)	log K_{sp}
H_2O		1000	18.1	1.0	3.0		
Ca_3SiO_5	C_3S	3210	72.4	0		10.0	0.477
C-S-H(m)	$C_3S_2H_3$	1750	100.0	0.001		0.29	-17.14
C-S-H(I)	CSH_4	2200	85.7	0.01		0.16	-6.92
C-S-H(II)	C_2SH_5	1850	161.2	0.75		0.019	-11.84
$Ca(OH)_2$		2240	33.08	0		32.3	-4.37
$Ca^{2+}_{(aq)}$					0.72		
$OH^-_{(aq)}$					5.28		
$H_2SiO_4^{2-}{}_{(aq)}$					0.70		

ρ is the density, V_m is the molar volume, the transport factor is defined to be the diffusion coefficient of mobile species in the material divided by their mobility in water, D_o is the diffusion coefficient at infinite dilution, k_{diss} is the forward rate constant for dissolution in water, and K_{sp} is the solubility product of the material. Where values are not given they are either not meaningful or were not used in the simulations. The values for certain parameters of the C-S-H phases, specifically their molar water content and the transport factors, are intended only as reasonable approximations. The water content both forms of stable C-S-H are likely too high, based on the analogous compositions of 1.4 nm tobermorite and jennite. However, the chosen values for the water content have little impact on the simulations when the pores are assumed to remain saturated, i.e., when water is replaced as rapidly as it is consumed by hydration reactions. Regarding the transport factors of C-S-H, we are aware of no independent experimental measurements of their values. In lieu of direct experimental tests of their values, we only note that the transport factors assumed here result in good overall fits to measured kinetic data on C_3S hydration reported by Garrault and Nonat (2001) and by Kondo and Ueda (1968)

C-S-H(m) and C-S-H(s), if assumed to be by a through-solution mechanism, will occur automatically if and when the solution reaches a proper level of supersaturation with respect to C-S-H(s). By adjusting the boundary conditions on the solution composition (i.e. pure water versus lime water), the water-solids ratio, and the particle size distribution of the cement particles, simulation results have been compared directly to experimental observations of the hydration rate and changes in solution chemistry. The reaction parameters and material properties are not all known, so they have been systematically varied to observe their predicted effects. The steady-state theory also has been tested by defining reaction parameters for adsorption of calcium and hydroxyl ions from solution and their effect on reducing the dissolution rate constant for the dissolving mineral. In keeping with the steady-state theory, no metastable form of C-S-H has been allowed in this case, but the composition, molar volume, porosity, and nucleation energy barrier for stable C-S-H is required. In this case, HydratiCA has been used to test whether or not the solution composition reaches the steady state, required by the steady-state theory, for any reasonable values of the rate constants for the various assumed reactions.

Through this kind of testing, a major result has been that neither the MBL theory nor the steady-state theory alone are likely able to account for the full range of experimental observations that have been made on C_3S hydration kinetics. Instead, a more plausible kinetic description, consistent with experiment, has been identified that incorporates certain aspects of both of these theories. Specifically, this new kinetic description involves composition-dependent nucleation and growth of a stable, but compositionally variable, form of C-S-H on the surface of C_3S particles (consistent with the steady-state theory), but mediated by the formation of a transient metastable hydrate that covers the C_3S particles at early times, sharply reduces the dissolution rate of C_3S, and establishes equilibrium with the surrounding pore solution (Bullard 2008).

Because this modeling approach is general, it can be expanded to address a number of other phenomena in cement-based materials besides hydration. For example, degradation of concrete by sulfate attack occurs by transport of ions from the boundary to the interior of the structure and subsequent reaction with existing phases to form new products that cause expansion strains and can lead to cracking. The rate of transport and of the sulfate reactions can be simulated directly on a digital-image representation of the 3-D microstructure using a model like HydratiCA. The predicted misfit of the reaction products at each point could be translated into a localized strain that could then be coupled to a finite element solver for digital images (Garboczi 1998) to determine the stress distribution and to identify regions susceptible to cracking. Alkali-silica reactions between cement paste and siliceous aggregates involve the same considerations and could be modeled using the same strategies since the underlying algorithms scale correctly to the greater length and time scales that would be involved.

A model that quantizes the concentration of individual components, as HydratiCA does, is ideally suited for linking to even more fundamental models at the molecular scale. Thus, for example, HydratiCA cannot predict *ab initio* the gel pore size distribution of C-S-H as a function of solution chemistry; instead it must assume a relation and simulate the consequences. But a suitably

formulated molecular dynamic model, using validated potential functions for C-S-H, might be able to predict this relation. If so, the upscaling of this information to HydratiCA would be straightforward.

5.4 Homogenization approach to modeling mechanical properties

Most civil engineering materials problems are multi-scale in nature because of inherent or induced heterogeneities existing at different length-scales. Inherent heterogeneities are those resulting from fluctuations in material properties such as diffusivity or strength. Induced heterogeneities are those imposed by a physical phenomenon (e.g., deformation) that alters the characteristics of the medium. For instance, **Fig. 13** and **Fig. 14** show typical scales relevant to granular and concrete-based materials, respectively. By comparing these figures, it is evident that granular materials have many parallel characteristics with cement-based materials; perhaps the most evident of which is the nanogranular structure of C-S-H at so-called 'level 0' (Ulm *et al.* 2004). All of the information pertaining to granular or nanogranular systems, including heterogeneities, is encoded at the granular scale and propagated or upscaled through to the macroscopic scales (e.g., level III, specimen scale, field scale, etc.).

The fundamental scale in these materials is the grain scale and hence models capable of representing the behavior at this scale would be fundamentally useful. However, accessing the granular scale (or level 0 in C-S-H) is computationally and analytically impossible at this point. Even teraflop computers cannot cope with the fact that the macroscopic response of granular materials is governed by particles rolling and sliding, expulsion of insterstitial fluids, and, at high pressures, grain comminution. However, as depicted in **Fig. 13**, the most interesting physics in engineering systems tends to occur in localized regions such as shear bands and cracks. Hence, models that probe the granular scale should focus on such regions where rich physics is occurring.

Unfortunately, modeling of deformation and failure in geomaterials such as soils, rocks, and concrete, has been tackled using mostly single-scale approaches. For example, many models have been proposed to capture deformation banding in granular materials (Andrade and Borja 2006, 2007, Borja and Andrade 2006, Cui and O'Sullivan 2006, O'Sullivan *et al.* 2003). Two broad methodologies can be identified: continuum models and discrete models. Continuum models traditionally rely on phenomenological laws designed to capture the macroscopic behavior of sands by smearing or averaging the granular-level processes, yielding relatively accurate stress-strain laws under relatively homogeneous deformations. Examples of continuum models can be found in the works of Andrade and Borja (2006), Bazant *et al.* (2000); Carner and Bazant (2000) and Gailly and Espinosa (2002). On the other hand, discrete models (which could include molecular dynamics models) are

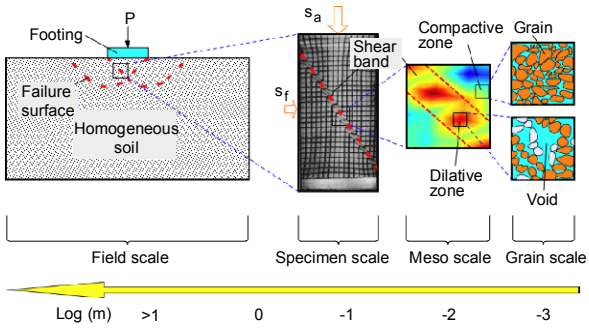

Fig. 13 Multi-scale nature of granular materials. After Andrade *et al*. (2007).

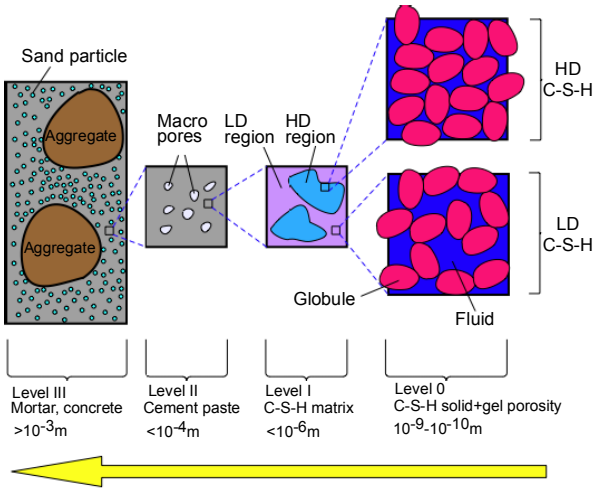

Fig. 14 Multi-scale nature of concrete-based materials.

predicated upon the fact that all processes in particulate media occur at the granular level and attempt to explicitly model inter-granular phenomena. By far the most popular discrete model is the so-called discrete element method (DEM) where grains are modeled as rigid bodies with or without inter-particle friction and cohesion (Cundall and Strack 1979, O'Sullivan *et al.* 2003, Tu and Andrade 2007). Unfortunately, both methodologies suffer from serious drawbacks: continuum models break down when forced to extrapolate outside of the phenomenological framework, whereas discrete models are computationally expensive at the macroscopic scale and require high-performance parallel computing to be predictive at such scales (Cundall 2001, Cleary *et al.* 2006).

To ameliorate the shortcomings of phenomenological models, several methodologies have been proposed. Homogenization is perhaps the most classic approach to obtaining effective properties in heterogeneous media. The idea behind homogenization is based on separation of the different homogeneous phases that comprise the heterogeneous media to obtain an equivalent homogeneous constitutive relation (Hill 1963, Hashin 1983, Zaoui 2002). Recently, these concepts have been applied in the area of poromechanics under the framework of

continuum micromechanics (Dormieux *et al*. 2002, Chateau and Dormieux 2002). Central to the idea of homogenization is the concept of representative elementa volume (REV) defined as the smallest possible region representative of the whole heterogeneous medium on average. In particular, homogenization has been used in obtaining the elastic properties in cement paste (Hashin and Monteiro 2002, Dormieux *et al*. 2004, Sanahuja *et al*. 2007) and in the multiscale investigation of poroelastic properties in C-S-H (Ulm *et al*. 2004).

A complementary alternative to classic homogenization is direct numerical simulation of heterogeneities via multiscale computation. Similar to classical homogenization, multiscale approaches were born as a method for obtaining constitutive responses without resorting to pure phenomenology. The pioneering Quasi-Continuum method proposed the use of the so-called Cauchy-Born rule to obtain a continuum energy density function from molecular dynamics computations within a finite region of interest (Tadmor *et al*. 1996). Another similar multiscale method is the recently proposed Virtual Power Domain Decomposition (Liu and McVeigh 2007), which has been used to do concurrent and hierarchical simulations in linear elastic solids with heterogeneities at multiple scales. Additionally, numerical homogenization of hardened cement paste, at a continuum level, has been performed using parameter identification and plasticity models (Hain and Wriggers 2007).

Multiscale simulation affords great flexibility and is not limited to applications where REVs are defined or to the use of linear elasticity. **Figure 15** shows an example of multiscale computations performed in granular materials. DEM computations are performed at the granular scale within a region of interest (say, within a shear band where the material behavior is unknown). Then, the DEM computations are used to upscale the behavior implied by the granular system by continuum computations using plasticity theories and the finite element method (FEM). In this fashion, as shown in **Fig. 15**, a continuum model is enriched by information obtained directly from granular scale computations while faithfully matching the material response implied by the granular system. The effective macroscopic parameters are obtained 'on the fly' and phenomenology is bypassed.

By the same token, it is clear from comparing **Fig. 13** and **Fig. 14** that the nano-globular structure of C-S-H is very similar to the microstructure of granular systems. Therefore, multiscale concepts developed for granular materials can be used to obtain a fundamental understanding of the behavior of C-S-H starting at the nanoscale, completely bypassing phenomenology at the macroscopic scale.

6. Present challenges and concluding remarks

One purpose of this paper is to discuss new approaches that might be used to develop a comprehensive and fundamental model of cement paste that simulates the development of structure at the nanoscale and microscale, and that can predict macroscale properties. Such a model, provided that it is based on fundamental chemical and physical principles, would have the important advantage of being capable of being extended to novel cements with a variety of starting compositions. This would, for example, streamline the process of designing and verifying new, greener, cement-based materials. Perhaps the most challenging aspect of a model of this type is to precisely and quantitatively define the pore system as a function of drying, mechanical loading, and other environmental factors. This understanding is the essence of the aging phenomenon that is central to constitutive models for creep and shrinkage.

There is evidence that the nanostructure is granular, with both elastic and viscous properties determined by particle contact and particle sliding. The details of the nanostructure are not easily investigated directly but rather must be inferred from multiple techniques, as shown in **Fig. 16**. The importance of nanostructure to elastic properties has now been reported in the literature (Constantinides and Ulm 2004, 2007). Both control of the nanostructure and detailed relationships to properties will require sophisticated mechanics models. In principle, the distribution of high-density C-S-H and low-density C-S-H should be taken into account to accurately predict elastic moduli over time as the microstructure develops (Smilauer and Bittnar 2006), although the assumption of constant average C-S-H elastic moduli has been used to make accurate predictions of the linear elastic properties of at least one OPC paste (Haecker *et al*. 2005). Even so, complex properties such as the nonlinear coupling of loading and drying (the Pickett effect), compressive strength, and propensity for cracking have not been explained on the microstructure level,

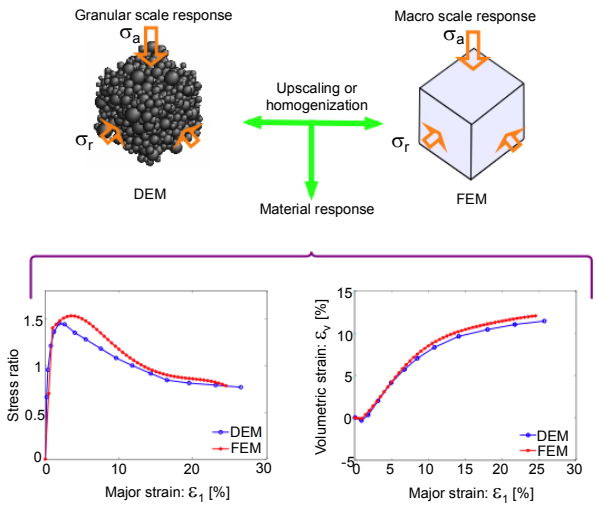

Fig. 15 Multiscale concept: from granular to macroscopic scale material responses.

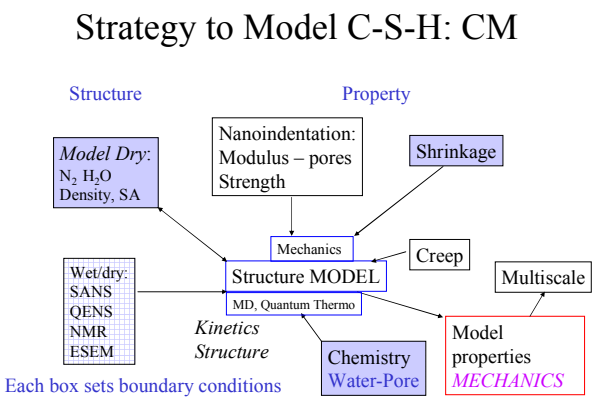

Fig. 16 The nanostructure of C-S-H is deduced by developing a model that is consistent with a number of observations. For example the size, surface area and distribution of particles is measured by SANS. Density and surface area are also determined by various adsorption and volumetric techniques. The distribution of particles must be consistent with kinetics of reaction. These results must reconcile with elastic properties determined by nanoindentation at the submicron scale, which is accomplished by multiscale mechanics. Molecular scale models are required to understand why the particles their specific size and properties, and ultimately control the nanostructure.

and there are certainly no detailed quantitative models yet available. This serves as an example of a great challenge.

To summarize, the following general observations can be made:

(1) The materials science approach – whereby an understanding of the fundamental links between processing, structure, and properties leads to predictive ability – is a valid and reasonable goal for cement based materials, and can lead to a new generation of powerful models. The success of these models may be judged on the basis of their ability to be extended to predict the structure and properties of new cementitious systems that are chemically and physically different from those used for the last hundred years.

(2) The nanostructure of cement paste, particularly its nanometer scale pore system, controls important bulk engineering properties, particularly for high-performance concretes where the capillary porosity is low and highly depercolated. Modern techniques are providing new information about the structure at this scale; however, much more remains to be learned regarding structural changes resulting from drying, application of load, changes in temperature, and various deterioration processes.

(3) Models will become more powerful as improved experimental measurements of cement paste nanostructure become available. While progress has been made on the size and distribution of nanoparticles that form under normal conditions, similar information is not available for systems that contain admixtures, especially mineral admixtures that change the chemistry of C-S-H, or for cements that react under extreme conditions. Because of the many variables, models must be based on the fundamental chemistry of the nanoparticles of C-S-H, including a thermodynamic description of what controls the size, shape, bonding between, and packing arrangement of the particles. The properties that are most challenging to model are those associated with creep, shrinkage, and the ingress of aggressive chemicals. Models of these properties require a detailed understanding of nanostructure, microstructure, and pores.

(4) The overall strategy to develop more powerful predictive models of concrete properties requires cooperative efforts from a variety of disciplines. The wedding of microstructure and mechanics holds particular promise. This will require coupling physicochemical models of the cement paste nanostructure with discrete granular mechanics and then upscaling to predict bulk properties. This provides a good example of how different disciplines and techniques must be combined if significant progress is to be made. At present, several fundamental issues have not been addressed with sufficient detail such that first principle models can be extended reliably into the realm of new cement-based materials.

Acknowledgment

This paper is part of a report for the Center of Advanced Cement Based Materials, headquartered at Northwestern University.

References

Allen, A. J. (1991). "Time-resolved phenomena in cements, clays and porous rocks." *Journal of Applied Crystallography*, 24, 624-634.

Allen, A. J., Thomas, J. J. and Jennings, H. M. (2007). "Composition and density of nanoscale calcium-silicate-hydrate in cement." *Nature Materials*, 6, 311-316.

Allen, A. J. and Thomas, J. J. (2007). "Analysis of C-S-H gel and cement paste by small-angle neutron scattering." *Cement and Concrete Research*, 37, 319-324.

Andrade, J. E. and Borja., R. I. (2006). "Capturing strain localization in dense sands with random density." *International Journal for Numerical Methods in Engineering*, 67, 1531–1564.

Andrade, J. E. and Borja., R. I. (2007). "Modeling deformation banding in dense and loose fluid-saturated sands." *Finite Elements in Analysis and Design*, 43, 361–383.

Andrade, J. E., Baker, J. W. and K. C. Ellison (2007). "Random porosity fields and their influence on the stability of granular media." *International Journal of Numerical and Analytical Methods in Geomechanics*,

in press.

Andrade, J. E., X. Tu and R. J. Finno (2008). "Multiscale framework for behavior prediction in granular media." *Mechanics of Materials*, in review.

Bangham, D. H. (1946). "The swelling and shrinkage of porous materials and the role of surface forces in determining technical strength." *Symposium Society Chemical Industry*.

Bazant, Z. P. (2001). "Creep of concrete." Encyclopedia of Materials: Science and Technology, B. Ilschner, ed., Elsevier.

Bazant, Z. P., Cusatis, G. and Cedolin, L. (2004). "Temperature effect on concrete creep modeled by microprestress-solidification theory." *Journal of Engineering Mechanics, ASCE,* 130(6), 691-699.

Bazant, Z. P., Caner, F. C., Carol, I., Adley, M. D. and Akers, S. A. (2000). "Microplane model M4 for concrete. I: Formulation with work-conjugate deviatoric stress." *Journal of Engineering Mechanics*,126, 944–953.

Beltzung, F. and Wittmann, F. H. (2005). "Role of disjoining pressure in cement based materials." *Cement and Concrete Research,* 35(12), 2364-2370.

Bentur, A., Milestone, N. B. and Young, J. F. (1978). "Creep and drying shrinkage of calcium silicate pastes II. induced microstructural and chemical changes." *Cement and Concrete Research,* 8, 721-732.

Bentz, D. P., Garboczi, E. J., Quenard, D. A., Baroghel-Bouny, V. and Jennings, H. M. (1995). "Modelling drying shrinkage in reconstructed porous materials. Part 1. Structural models from nanometers to millimeters." *Materials and Structures*, 28, 450-458.

Bentz, D. P. (1997). "Three-dimensional computer simulation of cement hydration and microstructure development." *Journal of the American Ceramic Society*, 80, 3-21.

Bentz, D. P., Garboczi, E. J. and Quenard, D. A. (1998). "Modelling drying shrinkage in reconstructed porous materials: application to porous vycor glass." *Modelling and Simulation in Materials Science and Engineering*, 6, 211-236.

Bentz, D. P., Mizell, S., Satterfield, S., Devaney, J., George, W., Ketcham, P., Graham, J., Porterfield, J., Quenard, D., Vallee, F., Sallee, H., Boller, E. and Baruchel, J. (2002). "The Visible Cement Data Set." *Journal of Research of the National Institute of Standards and Technology*, 107, 137-148.

Bentz, D. P. (2007). "Cement hydration: building bridges and dams at the microstructure level." *Materials and Structures*, 40, 397-404.

Bentz, D. P. and Martys, N. S. (2007). "A Stokes permeability solver for three-dimensional porous media." NIST Interagency Report 7416. U.S. Department of Commerce.

Bonaccorsi, E., Merlino, S. and Kampf, A. R. (2005). "The crystal structure of Tobermorite 14 Å (Plombierite), a C-S-H Phase." *Journal of the American Ceramic Society*, 88, 505-512.

Bonaccorsi, E., Merlino, S. and Taylor, H. F. W. (2004). "The crystal structure of jennite, $Ca_9Si_6O_{18}(OH)_6 \cdot 8H_2O$." *Cement and Concrete Research*, 34, 1481-1488.

Borja, R. I. and Andrade, J. E. (2006). "Critical state plasticity, Part VI: Meso-scale finite element simulation of strain localization in discrete granular materials." *Computer Methods in Applied Mechanics and Engineering*, 195, 5115–5140.

van Breugel, K. (1991). "Simulation of hydration and formation of structure in hardening cement-based materials." Ph.D. thesis, Delft University of Technology, Delft, The Netherlands.

Brunauer, S., Emmett, P. H. and Teller, E. (1938). "Adsorption of gases in multimolecular layers." *Journal of the American Chemical Society* 60, 309-319.

Brunauer, S. (1972). "Further discussion of the helium flow results of R. F. Feldman." *Cement and Concrete Research*, 2, 749-753.

Bullard, J. W., Ferraris, C., Garboczi, E. J., Martys, N. and Stutzman, P. (2004). "Virtual cement." *Innovations In Portland Cement Manufacturing*. J.I. Bhatty, F.M. Miller and S.H. Kosmatka, eds., Portland Cement Association, Skokie, IL, 1311-1331.

Bullard, J. W. (2007a). "Approximate rate constants for nonideal diffusion and their application in a stochastic model." *Journal of Physical Chemistry A*, 111, 2084-2092.

Bullard, J. W. (2007b). "A three-dimensional microstructural model of reactions and transport in aqueous mineral systems." *Modelling and Simulation in Materials Science and Engineering*, 15, 711-738.

Bullard, J. W. (2008). "A determination of hydration mechanisms for tricalcium silicate using a kinetic cellular automaton model," submitted to the *Journal of the American Ceramic Society*.

Bullard, J. W. and Garboczi, E. J. (2006). "A model investigation of the influence of particle shape on Portland cement hydration." *Cement and Concrete Research.* 36, 1007-1015.

Cahn, J. W. (1956). "The kinetics of grain boundary nucleated reactions." *Acta Metallurgica*, 4, 449-459.

Caner, F. C. and Ba˘zant, Z. P. (2000). "Microplane model M4 for concrete. II: Algorithm and calibration." *Journal of Engineering Mechanics*, 126, 954–961.

Chateau, X. and Dormieux, L. (2002). "Micromechanics of saturated and unsaturated porous media." *International Journal for Numerical and Analytical Methods in Geomechanics*, 26, 831–844.

Chen, J. J., Thomas, J. J., Taylor, H. F. W. and Jennings, H. M. (2004). "Solubility and structure of calcium silicate hydrate." *Cement and Concrete Research*, 34, 1499-1519.

Chen, J. J., Thomas, J. J. and Jennings, H. M. (2006). "Decalcification shrinkage of cement paste." *Cement and Concrete Research,* 36(5), 801-809.

Cleary, P. W., Morrison, R. and Sinnott, M. (2006). "Progress in DEM modeling of comminution related unit processes: screens, crushers and mills." *International Conference on Mineral Processing XXIII*. G. Onal *et al*., eds. 1794-1799.

Constantinides, G. and Ulm, F.-J. (2004). "The effect of two types of C-S-H on the elasticity of cement-based materials: results from nanoindentation and micromechanical modeling." *Cement and Concrete Research*, 34(1), 67-80.

Constantinides, G. and Ulm, F.-J. (2007). "The nanogranular nature of C-S-H." *Journal of the Mechanics and Physics of Solids*, 55, 64-90.

Coussy, O., Dangla, P., Lassabatere, T. and Baroghel-Bouny, V. (2004). "The equivalent pore pressure and the swelling and shrinkage of cement based materials," *Materials and Structures*, 37, 15-20.

Cui, L. and O'Sullivan, C. (2006). "Exploring the macro- and micro-scale response of an idealized granular material in the direct shear apparatus." *Geotechnique*, 56, 455–468.

Cundall, P. A and Strack, O. D. L. (1979). "A discrete numerical model for granular assemblies." *Geotechnique*, 29, 47–65.

Cundall, P. A. (2001). "A discontinuous future for numerical modelling in geomechanics?" *Geotechnical Engineering, ICE*, 149, 41–47.

Damidot, D., Nonat, A. and Barret, P. (1990). "Kinetics of tricalcium silicate hydration in diluted suspensions by microcalorimetric measurements." *Journal of the American Ceramic Society*, 73, 3319-3320.

Damidot, D., Bellmann, F., Möser, B. and Sovoidnich, T. (2007). "Calculation of the dissolution rate of tricalcium silicate in several electrolyte solutions." *Cement-Wapno-Beton*, 12/74, 57-67.

Damtoft, J. S., Lukasik, J., Herfort, D., Sorrentino, D. and Gartner, E. M. (2008). "Sustainable development and climate change initiatives." *Cement and Concrete Research,* in press.

Darken, L. S. and Gurry, R. W. (1953). *Physical Chemistry of Metals*. McGraw-Hill, New York.

Diamond, S. and Bonen, D. (1993). "Microstructure of hardened cement paste--A new interpretation." *Journal of the American Ceramic Society*, 76, 2993-2999.

Dormieux, L., Molinari, A. and Kondo, D. (2002). "Micromechanical approach to the behavior of poroelastic materials." *Journal of the Mechanics and Physics of Solids*, 50, 2203–2231.

Dormieux, L., Lemarchand, E., Kondo, D. and Fairbairn, E. (2004). "Elements of poro-micromechanics applied to concrete." *Materials & Structures*, 37, 31–42.

Farmer, V. C., Jeevaratnam, J., Speakman, K. and Taylor, H. F. W. (1966). "Thermal decomposition of 14 Å Tobermorite from Crestmore." *Symposium on Structure of Portland Cement Paste and Concrete*, Washington, DC, 291-2999.

Feldman, R. F. (1971). "The flow of helium into the interlayer spaces of hydrated Portland cement paste." *Cement and Concrete Research*, 1, 285 - 300.

Feldman, R. F. and Sereda, P. J. (1968). "A model for hydrated Portland cement paste as deduced from sorption-length change and mechanical properties." *Materials and Structures,* 1(6), 509-520.

Feret. R. (1897). *Bulletin de Société d'Encouragement pour l'Industrie Nationale Paris* 2, 1604.

Gailly, B. A. and Espinosa, H. D. (2002). "Modelling of failure mode transition in ballistic penetration with continuum model describing microcracking and flow of pulverized media." *International Journal for Numerical Methods in Engineering*, 54, 365–398.

Garboczi, E. J. (1998). "Finite element and finite difference programs for computing the linear electric and elastic properties of digital images of random materials." NIST Interagency Report 6269. U.S. Department of Commerce.

Garboczi, E. J. and Bentz, D. P. (2001). "The effect of statistical fluctuation, finite size error and digital resolution on the phase percolation and transport properties of the NIST cement hydration model." *Cement and Concrete Research*, 31, 1501-1514.

Garrault-Gauffinet, S. and Nonat, A. (1999). "Experimental investigation of calcium silicate hydrate (C-S-H) nucleation." *Journal of Crystal Growth*, 200, 565-574.

Garrault, S. and Nonat, A. (2001). "Hydrated layer formation on tricalcium and dicalcium silicate surfaces: Experimental study and numerical simulations." *Langmuir,* 17, 8131-8138.

Garrett, G. G., Jennings, H. M. and Tait, R. B. (1979). "The fatigue hardening behaviour of cement-based materials." *Journal of Materials Science,* 14, 296-306.

Gartner, E. M. and Gaidis, J. M. (1989). "Hydration mechanisms, I." *Materials Science of Concrete*, The American Ceramic Society, Westerville, OH, 95-125.

Gartner, E. M. (2004). "Industrially interesting approaches to "low-CO_2" cements." *Cement and Concrete Research*, 34, 1489-1498.

Glasstone, S., Laidler, K. J. and Eyring, H. (1941). *The Theory of Rate Processes.* McGraw-Hill, New York.

Haecker, C. J., Garboczi, E. J., Bullard, J. W., Bohn, R. B., Sun, Z., Shah, S. P. and Voigt, T. (2005). "Modeling the linear elastic properties of Portland cement paste." *Cement and Concrete Research*, 35, 1948-1960.

Hain, M. and Wriggers, P. (2008). "Numerical homogenization of hardened cement paste." *Computational Mechanics*, In press.

Halperin, W. P., Jehng, J. Y. and Song, Y. Q. (1994). "Application of spin-spin relaxation to measurement of surface area and pore size distributions in a hydrating cement paste." *Magnetic Resonance Imaging*, 12, 169-173.

Harned, H. W. and Owen, B. B. (1958). *The Physical Chemistry of Electrolytic Solutions*. *3rd Edition*. Reinhold Publishing, New York.

Hashin, Z. (1983). "Analysis of composite materials—A survey." *Journal of Applied Mechanics*, 50, 481–505.

Hashin, Z. and Monteiro, P. J. M. (2002). "An inverse method to determine the elastic properties of the interphase between the aggregate and the cement paste." *Cement and Concrete Research*, 32, 1291–1300, 2002.

Hill, R. (1963). "Elastic properties of reinforced solids: some theoretical principles." *Journal of the Mechanics and Physics of Solids*, 11, 357–372.

Holzer, L., Muench B., Wegmann M., Gasser, P. and Flatt, R. J. (2006). "FIB-nanotomography of particulate systems - Part I: Particle shape and topology of interfaces." *Journal of the American Ceramic Society,* 89, 2577-2585.

Jennings, H. M., Dangleish, B. J. and Pratt, P. L. (1981). "Morphological development of hydrating tricalcium silicate as examined by electron microscopy techniques." *Journal of the American Ceramic Society*, 64(10), 567-572.

Jennings, H. M. and Johnson, S. K. (1986). "Simulation of microstructure development during the hydration of a cement compound." *Journal of the American Ceramic Society*, 69, 790-795.

Jennings, H. M. and Tennis, P. D. (1994). "Model for the developing microstructure in Portland cement pastes." *Journal of the American Ceramic Society,* 77(12), 3161-3172.

Jennings, H. M. (2000). "A model for the microstructure of calcium silicate hydrate in cement paste." *Cement and Concrete Research*, 30, 101-116.

Jennings, H. M. (2004). "Colloid model of C-S-H and implications to the problem of creep and shrinkage." *Mater. Struct./Concr. Sci. Engrg.,* 37, 59-70.

Jennings, H. M., Thomas, J. J., Gevrenov, J. S., Constantinides, G. and Ulm, F.-J. (2007). "A multi-technique investigation of the nanoporosity of cement paste." *Cement and Concrete Research*, 37, 329-336.

Jennings, H. M. (2008). "Refinments to colloid model of C-S-H in cement: CMII." *Cement and Concrete Research,* in press.

Kak, A. C. and Slaney, M. (2001). *Principles of Computerized Tomographic Imaging*. Society for Industrial and Applied Mathematics, Philadelphia, PA.

Kondo, R. and Ueda S. (1968). "Kinetics and Mechanisms of the Hydration of Cements." *Proceedings of the Fifth International Symposium on the Chemistry of Cement, II, Hydration of Cements, Tokyo, Japan.* Volume 2, 203-212.

Korb, J. P., Monteilhet, L., McDonald, P. J. and Mitchell, J. (2007). "Microstructure and texture of hydrated cement-based materials: A proton field cycling relaxometry approach." *Cement and Concrete Research*, 37(3), 295-302.

Liu, W. K. and McVeigh, C. (2008). "Predictive multiscale theory for design of heterogeneous materials." *Computational Mechanics*. Submitted.

Mackenzie, J. K. (1950). "The elastic constants of a solid containing spherical holes." *Proceedings of the Physical Society*, 683, 2-11.

McDonald, P. J., Korb, J. P., Mitchell, J. and Monteilhet, L. (2005). "Surface relaxation and chemical exchange in hydrating cement pastes: A two-dimensional NMR relaxation study." *Physical Review E*, 72, 011409.

McDonald, P. J., Mitchell, J., Mulheron, M., Monteilhet, L. and Korb, J. P. (2007). "Two-dimensional correlation relaxation studies of cement pastes." *Magnetic Resonance Imaging*, 25(4), 470-473.

Merlino, S., Bonaccorsi, E. and Armbruster, T. (1999). "Tobermorites: Their real structure and order-disorder (OD) character." *American Mineralogist*, 84, 1613-1621.

Mills, R. and Lobo, V.M.M. (1989). *Self-Diffusion in Electrolyte Solutions*. Elsevier, Amsterdam.

Mitsuda, T. and Taylor, H. F. W. (1978). "Normal and anomalous tobermorites." *Mineral Magazine*, 42, 229-235.

Monteilheit, L., Korb, J.-P,, Mitchell, J. and McDonald, P. J. (2006). "Observation of exchange of micro-pore water in cement pastes by 2-dimensional $T_2 - T_2$ nuclear magnetic resonance relaxometry." *Physical Review E*, 74:061404.

Neubauer, C. M. and Jennings, H. M. (2000). "The use of digital images to determine deformation throughout a microstructure, Part II: Application to cement paste." *Journal of Materials Science,* 35(22), 5751-5765.

Nonat, A. (2004). "The structure and stoichiometry of C-S-H.." *Cement and Concrete Research,* 34, 1521-1528.

O'Sullivan, C. J., Bray, D. and Li., S. (2003). "A new approach for calculating strain for particulate media." *International Journal for Numerical and Analytical Methods in Geomechanics*, 27, 859–877.

Powers, T. C. (1958). "Structure and physical properties of hardened portland cement paste." *Journal of the American Ceramic Society,* 41, 1-6.

Powers, T. C. (1959). "Capillary continuity or discontinuity in cement paste." *Portland Cement Association Bulletin,* 10, 2-12.

Powers, T. C. (1960). "Physical properties of cement paste." *Fourth International Symposium on the Chemistry of Cement, Washington,* D. C., 577-609.

Powers, T. C. (1968). "The thermodynamics of volume change and creep." *Materiaux et Constructions*, 1(6), 487-507.

Powers, T. C. and Brownyard, T. L. (1948) "Studies of the physical properties of hardened Portland cement paste." *PCA Bulletin* 22.

Powers, T. C., Copeland, L. E., Hayes, J. C. and Mann, H. M. (1955) "Permeability of Portland cement caste." *Journal of the American Concrete Institute*, 51, 285-298.

Ramachandran, V. S., Feldman, R. F. and Beaudoin, J. J. (1981). *Concrete Science,* Heyden, London.

Richardson, I. G. (2002). "Electron microscopy of

cements." Chapter 22 in Structure and Performance of Cements, 2nd ed., P. Barnes and J. Bensted, eds., Spon Press, London, 500-556.

Richardson, I. G. (2004). "Tobermorite/jennite- and tobermorite/calcium hydroxide-based models for the structure of C-S-H: applicability to hardened pastes of tricalcium silicate, -dicalcium silicate, Portland cement and blends of Portland cement with blast-furnace slag, metakaolin, or silica fume." *Cement and Concrete Research*, 34, 1733-1777.

Ryshkewitch, E. (1953). "Compression strength of porous sintered alumina and zirconia." *Journal of the American Ceramic Society*, 36, 65-68.

Sanahuja, J., Dormieux, L. and Chanvillard, G. (2007). "Modelling Elasticity of a Hydrating Cement Paste." *Cement & Concrete Composites*, 37, 1427-1438.

Scherer, G. W., Valenza II, J. J.. and Simmons, G. (2007). "New methods to measure liquid permeability in porous materials." *Cement and Concrete Research,* 37, 386-397.

Smilauer, V. and Bittnar, Z. (2006). "Microstructure-based micromechanical prediction of elastic properties in hydrating cement paste." *Cement & Concrete Composites,* 36, 1708-1718.

Stein, H. N. and Stevels, J. M. (1964). "Influence of silica on the hydration of $3CaO.SiO_2$." *Journal of Applied Chemistry*, 14, 338-346.

Tadmor, E., Ortiz, M. and Phillips, R. (1996). "Quasicontinuum analysis of defects in solids." *Philosophical Magazine A*, 73, 1529–1563.

Taylor, H. F. W. (1950). "Hydrated calcium silicates. Part I. Compound formation at ordinary temperatures." *J. Chem. Soc.*, 3682-3690.

Taylor, H. F. W. (1961). "The chemistry of cement hydration (Chapter 3)." *Progress in Ceramic Science,* J. E. Burke, ed., Pergamon Press, New York, 89-145.

Taylor, H. F. W. (1968) "The calcium silicate hydrates." *Proc. 5th Int. Symp. Chem. Cem.*, Tokyo, Japan, 1-26.

Taylor, H. F. W. (1986). "Proposed structure for calcium silicate hydrate gel." *Journal of the American Ceramic Society*, 69, 464-467.

Taylor, H. F. W. (1997). *Cement Chemistry, 2nd Ed.*, Thomas Telford, London.

Tennis, P. D. and Jennings, H. M. (2000). "A model for two types of calcium silicate hydrate in the microstructure of Portland cement pastes." *Cement and Concrete Research,* 30(6), 855-863.

Thomas, J. J. (2007). "A new approach to modeling the nucleation and growth kinetics of tricalcium silicate hydration." Journal of the American Ceramic Society, 90, 3282-3288.

Thomas, J. J. and Jennings, H. M. (1999). "Effects of D2O and mixing on the early hydration kinetics of tricalcium silicate." Chemistry of Materials, 11, 1907-1914.

Thomas, J. J. and Jennings, H. M. (2002). "Effect of heat treatment on the pore structure and drying shrinkage behavior of hydrated cement paste." Journal of the American Ceramic Society, 85(9), 2293-98.

Thomas, J. J. and Jennings, H. M. (2006). "A colloidal interpretation of chemical aging of the C-S-H gel and its effects on the properties of cement paste." Cement and Concrete Research, 36, 30-38.

Thomas, J. J., Jennings, H. M. and Allen, A. J. (1998). "The surface area of cement paste as measured by neutron scattering - Evidence for two C-S-H morphologies." Cement and Concrete Research, 28(6), 897-905.

Thomas, J. J., Jennings, H. M. and Allen, A. J. (1999). "The surface area of hardened cement paste as measured by various techniques." Concrete Science and Engineering, 1, 45-64.

Thomas, J. J., Allen, A. J. and Jennings, H. M. (2007a). "Structural changes to the calcium silicate hydrate gel phase of hydrated cement on aging, drying and resaturation." (In preparation).

Thomas, J. J., Jennings, H. M. and Chen, J. J. (2008). "Acceleration of the hydration kinetics of C_3S and cement paste by seeding." (In preparation).

Tu, X. and Andrade, J. E. (2007). "Criteria for static equilibrium in particulate mechanics computations." *International Journal for Numerical Methods in Engineering*, Submitted.

Ulm, F.-J., Constantinides, G. and Heukamp, F. H. (2004). "Is concrete a poromechanics material? - A multiscale investigation of poroelastic properties." *Materials and Structures*, 37, 43-58.

van't Hoff, H. (1903). *Vorlesungen über Thoretische und Physakalische Chemie*. Braunschweig, Berlin, Germany.

Vichit-Vadakan, W. and Scherer, G. W. (2000)(2004). "Measuring permeability of rigid materials by a beam-bending bethod: II. Porous Vycor." *Journal of American Ceramamic Socociety*, 83, 2240-2245; *Erratum, Journal American Ceramic Society*, 87, 1614.

Vlahinic, I., Jennings, H. and Thomas, J. (2008). "A constitutive model for drying and shrinkage of partially saturated drying porous material." (In preparation).

Wittmann, F. (1970). "Einfluss des feuchtigkeitsgehaltes auf das kriechen des zementsteines." *Rheologica Acta,* 9, 282 - 287.

Wittmann, F. H. (1979) "Trends in research on creep and shrinkage of concrete." *Cement Production and Use,* New Hampshire, 143-161.

Zaoui, A. (2002). "Continuum micromechanics: Survey." *Journal of Engineering Mechanics*, 128, 808–816.